SAND2011-0200C
11PFL-0806

Boosted HCCI – Controlling Pressure-Rise Rates for Performance Improvements using Partial Fuel Stratification with Conventional Gasoline

John E. Dec, Yi Yang, and Nicolas Dronniou
Sandia National Laboratories

ABSTRACT

This study investigates the potential of partial fuel stratification for reducing the knocking propensity of intake-boosted HCCI engines operating on conventional gasoline. Although intake boosting can substantially increase the high-load capability of HCCI, these engines would be more production-viable if the knock/stability load limit could be extended to allow higher loads at a given boost and/or to provide even higher thermal efficiencies. A technique termed partial fuel stratification (PFS) has recently been shown to greatly reduce the combustion-induced pressure-rise rate (PRR), and therefore the knocking propensity of naturally aspirated HCCI, when the engine is fueled with a ϕ-sensitive, two-stage-ignition fuel. The current work explores the potential of applying PFS to boosted HCCI operation using conventional gasoline, which does not typically show two-stage ignition. Experiments were conducted in a single-cylinder HCCI research engine (0.98 liters) at 1200 rpm. The engine was equipped with a compression-ratio 14 piston, and combustion phasing was controlled by EGR addition.

PFS is produced by premixing the majority of the fuel and then directly injecting the remainder (up to about 20%) in the latter part of the compression stroke. For PFS to be effective, the fuel's autoignition chemistry must vary with the local equivalence ratio (ϕ) to produce a staged combustion event. Accordingly, tests were conducted to determine the ϕ-sensitivity of gasoline. They show that at naturally aspirated conditions (P_{in} = 1 bar), gasoline is not ϕ-sensitive, and PFS is not effective for reducing the PRR. However, with sufficient intake boost (*e.g.* P_{in} = 2 bar), gasoline is found to become highly ϕ-sensitive, and PFS very effectively reduces the PRR. Varying the amount of PFS, by adjusting either the timing or amount of DI fuel, allows control of the PRR reduction. Applying PFS to high loads at P_{in} = 2 bar substantially shifts the knock/stability limit and increases the maximum $IMEP_g$ from 11.7 (premixed) to 13.0 bar (PFS). Maximum load improvements with PFS are also seen for other intake pressures ranging from 1.6 to 2.4 bar. Finally, because it allows more advanced combustion phasing without knock, PFS is also effective for increasing the thermal efficiency of boosted HCCI over a range of loads for each P_{in}, yielding typical fuel economy improvements of 2 – 2.5%. Overall, PFS has a strong potential for improving gasoline-fueled boosted HCCI operation.

INTRODUCTION

Concerns about limited petroleum supplies, global warming, and urban air pollution are driving the demand for engines that are both highly fuel efficient and have low levels of toxic emissions. At the same time, significant market penetration requires that cost of these improvements be minimal. Homogeneous Charge Compression Ignition (HCCI) and HCCI-like combustion has been shown to be capable of providing high thermal efficiencies and ultra-low NOx and particulate matter (PM) emissions, using relatively inexpensive gasoline spark-ignition (SI) engine fuel injectors. These features make HCCI well suited for future transportation engines; however, the limited power output of these engines still remains a barrier to their widespread implementation.

The load limitation typically occurs because the maximum cylinder-pressure rise rate (PRR) increases with fueling rate, eventually causing engine knock. To mitigate these high PRRs with increased fueling, the combustion phasing can be retarded, but the amount of allowable retard is limited by excessive cycle-to-cycle variation in the power output, and eventually misfire [1,2]. As the fueling is increased, it can become increasingly difficult to maintain sufficiently retarded combustion to prevent run-away knock [3] without having poor combustion stability that can drift into misfire [1,2,4]. Closed-loop control systems can help extend this knock/stability limit [1], but the maximum load for naturally aspirated HCCI remains low relative to traditional spark-ignition or turbo-charged diesel engines.

INTAKE-BOOSTED HCCI

Intake-pressure boosting is often used to increase the power output of internal combustion engines, and for HCCI engines, it provides a means of increasing the power while still maintaining a sufficiently dilute charge to prevent NOx formation. However, early efforts with intake-boosted HCCI met with limited success due to difficulties in controlling engine knock. The knocking propensity of HCCI increases with boost because the greater charge mass with boost results in a greater pressure rise with combustion, and because boost enhances the autoignition process causing the combustion phasing to advance. As a result, most early attempts to achieve high loads with boosted HCCI used special fuels and/or reduced compression ratios [5-8].

Recently, however, the authors demonstrated that substantial increases in the high-load limit of HCCI could be achieved with intake pressure boosting using conventional gasoline and a compression ratio of 14 [9]. In this previous work, the maximum load attainable increased substantially with boost, up to the highest load attempted, a gross indicated mean effective pressure ($IMEP_g$)[1] = 16.3 bar at P_{in} = 325 kPa. For all conditions, fully premixed fueling was used, NOx emissions were very low, PM was not detectable, and PRRs were kept sufficiently low to prevent engine knock. Controlling the PRR under highly boosted conditions required substantial combustion-phasing retard. Fortunately, for boosted operation with gasoline fueling, good combustion stability could be maintained at much later combustion phasings than was possible for naturally aspirated operation, due to an enhancement of the intermediate-temperature reactions that occur prior to full hot ignition, as discussed in detail in Ref. [9]. To achieve the required retard despite the pressure-induced enhancement of autoignition, a combination of reduced intake temperature and cooled EGR was used.

---

[1] $IMEP_g$ refers to the IMEP over the compression and expansion strokes only, while $IMEP_{net}$ refers to the IMEP over the entire cycle, including the gas-exchange strokes.

Although these previous results [9] show the strong potential of boosted HCCI with gasoline fueling, there are still several aspects where improvements are desirable. Three key areas are: 1) For boost levels below $P_{in} \approx 260$ kPa, the load is limited by the knock/stability limit.[2] If the combustion PRR could be reduced by some means other than timing retard, the reduced knocking propensity could shift the knock/stability limit or remove it altogether, thus allowing higher fueling rates at these boost levels. 2) Exhaust enthalpies, although adequate, are lower than desirable for driving a turbo-charger. Increasing the load for a given boost would increase exhaust temperatures, easing turbo-charger design. 3) Although the thermal efficiencies reported in [9] are high, even higher thermal efficiencies could be obtained if less timing retard was required to control knock.

PARTIAL FUEL STRATIFICATION

One promising method for controlling the combustion heat release rate (HRR) and hence, the combustion PRR in HCCI engines to use partial fuel stratification. However, for fuel stratification to reduce the HRR, autoignition times must be sensitive to variations in the local fuel/air equivalence ratio (ϕ), so that the ϕ-stratification produces a staged heat release event [10] as autoignition occurs sequentially down the ϕ gradient. Using a special technique to isolate fuel-chemistry effects from thermal effects, Dec and Sjöberg [11] showed that the autoignition chemistry of some fuels is sensitive to variations in ϕ (ϕ-sensitive) while for other fuels variations in ϕ have little or no effect on the autoignition delay times. They showed that PRF80, which exhibited two-stage ignition at the conditions studied, showed significant ϕ-sensitivity, while iso-octane and gasoline, which exhibited single-stage ignition were <u>not</u> ϕ-sensitive at these naturally aspirated conditions. Subsequently, Sjöberg and Dec [10] demonstrated that the ϕ-sensitivity of PRF83, which showed two-stage ignition at the conditions studied, could be exploited to reduce the HRR of a naturally aspirated HCCI engine. To accomplish this, they used a mixture preparation technique dubbed partial fuel stratification (PFS), in which the majority of the fuel is premixed and a fraction (up to about 20%) is directly injected during the latter part of the compression stroke using a gasoline-type direct injector (GDI) to provide the mixture stratification. As discussed in Ref. [10], this PFS technique was chosen because computations indicated that it could provide more than enough fuel stratification, and the premixed fuel maintains a sufficiently high ϕ in the leanest parts of the charge to obtain good combustion efficiency [12]. The large premixed portion also assures good air utilization throughout the combustion chamber.

Later, the current authors conducted a more in-depth study of the potential of PFS to reduce HRRs of HCCI [13]. This work showed that a two-stage-ignition fuel with stronger pre-ignition reactions (*i.e.* reactions that occur at low and intermediate temperatures prior to hot ignition), PRF73, was very effective at reducing the HRR at a high-load operating point while maintaining clean (low NOx), efficient, and stable HCCI combustion. This work also showed that a single-stage-ignition fuel, iso-octane, showed no tendency to reduce the HRR. Finally, in a work concurrent with the study presented here, the authors showed that a distillate fuel with two-stage ignition and an overall HCCI autoignition reactivity similar to PRF73 was also very effective at reducing the HRR with PFS [14]. These results are consistent with other works in the literature. Dahl *et al.* [15] showed that the PRR of a two-stage fuel (RON ~ 50) was reduced with mixture stratification more

[2] For $P_{in} \geq 260$, the maximum load is limited by oxygen availability because of the high EGR levels required to control combustion phasing, so reductions in the PRR will not allow higher loads unless they also reduce EGR requirements.

effectively than with a RON = 100 gasoline in a high residual engine utilizing negative valve overlap. Wada and Senda [16] found that mixture stratification produced a larger reduction in PRR with a fuel showing a strong low-temperature heat release (LTHR), PRF45, than did a fuel with weak LTHR, PRF80. All of these previous studies were at naturally aspirated conditions.

These previous works consistently show that mixture stratification is effective for reducing the HRR for fuels having two-stage ignition, and it is ineffective for fuels with single-stage ignition. Additionally, they indicate that two-stage fuels having stronger LTHR are more effective than those with less. Generalizing, fuels that have greater HCCI autoignition reactivity (*i.e.* that autoignite more easily under HCCI conditions) are more likely to have a higher ϕ-sensitivity and to be more effective for use with mixture stratification than those with lower autoignition reactivity.

Gasoline is designed to have a low autoignition reactivity (high octane number), and it has been shown to be a single-stage ignition fuel at typical naturally aspirated HCCI operating conditions [9,17], which suggests that it will not be effective with mixture stratification. However, intake-pressure boosting enhances autoignition reactivity of gasoline significantly [9]. Most of this enhancement of the pre-ignition reactions is in the form of increased intermediate-temperature heat release (ITHR) with significant LTHR being evident only at the lowest intake temperature (T_{in}) tested, 45°C. Although it is strictly speaking still a single-stage fuel (or nearly single-stage) at most of the boosted conditions presented in our previous study of boosted HCCI [9], the substantial increase in autoignition reactivity suggests that gasoline may still become ϕ-sensitive under boosted conditions, allowing the use of PFS to reduce the heat release rate.

OBJECTIVES

The objective of the current work is to examine the potential for using mixture stratification to improve boosted HCCI operation with conventional gasoline. The results of this study are presented in four parts:

1. Examination of the ϕ-sensitivity of gasoline for naturally aspirated and boosted HCCI operation.

2. Investigation of the effects of PFS on the PRR and HRR at a selected high-load fueling rate for naturally aspirated (1 bar) and boosted (2 bar) operation. To determine how the effectiveness of PFS changes with the amount of stratification, sweeps of both the direct-injection (DI) timing and the DI fraction are conducted for both intake pressures.

3. Application of PFS to determine the extent to which the high-load limit of boosted HCCI can be extended for a range of boost levels from 1.6 – 2.4 bar absolute.

4. Investigation of the potential of using PFS to improve the efficiency of boosted HCCI by allowing more advanced combustion phasing without knock.

EXPERIMENTAL SETUP & DATA ACQUISITION

ENGINE FACILITY

The HCCI research engine used for this study was derived from a Cummins B-series six-cylinder diesel engine, which is a typical medium-duty diesel engine with a displacement of 0.98 liters/cylinder. Figure 1 shows a schematic of the engine, which has been converted for single-cylinder operation by deactivating cylinders 1–5. The engine specifications and operating

conditions are listed in Table 1. The configuration of the engine and facility are identical to those used our previous study of intake pressure boost [9]. Additional information on the facility may be found in Ref. [3,12].

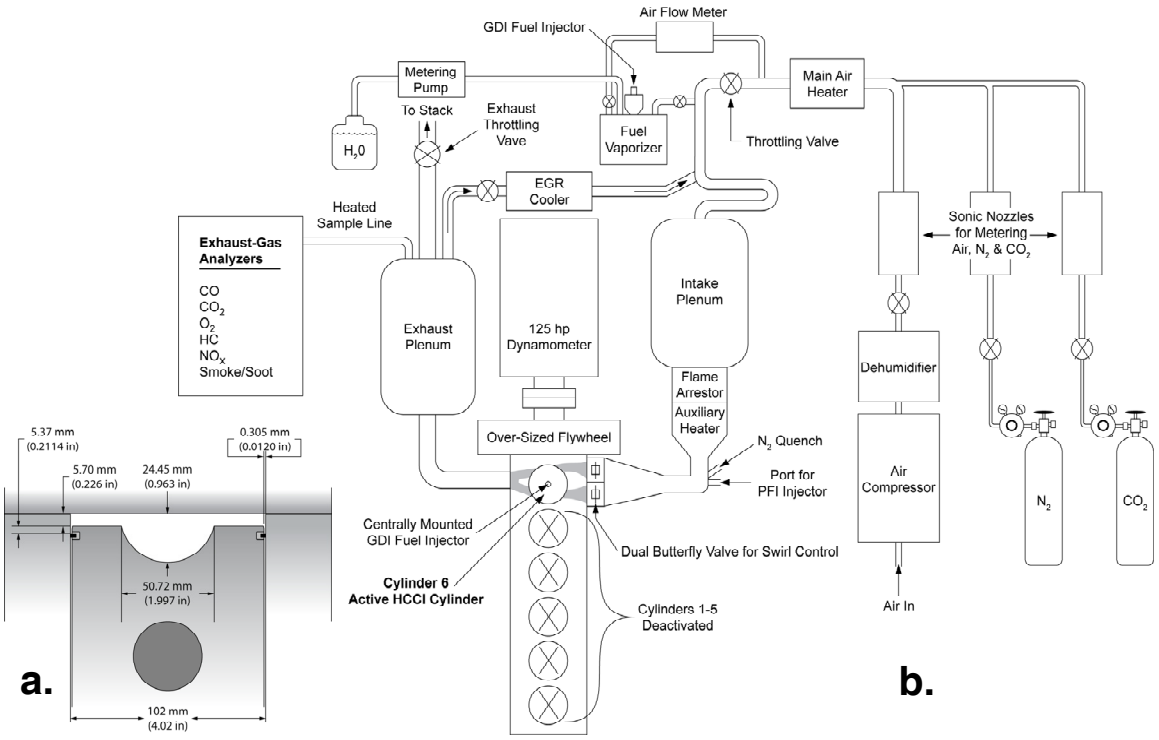

Figure 1. Schematic of the HCCI engine facility (b), and combustion chamber geometry of the CR = 14 piston, at TDC (a).

The active HCCI cylinder is fitted with a compression-ratio (CR) = 14 custom piston as shown in Fig. 1a. This piston provides an open combustion chamber with a large squish clearance and a quasi-hemispherical bowl. Comparison tests showed minimal differences in performance and emissions compared to the CR = 14 broad shallower-bowl piston used in many earlier studies *e.g.* [4,18]. Both pistons provide a small topland ring crevice, amounting to only 2.1% of the top-dead-center (TDC) volume. A more complete discussion of the comparison between pistons may be found in Ref. [3].

TABLE 1. Engine Specifications and Operating Conditions

Displacement (single-cylinder)	0.981 liters
Bore	102 mm
Stroke	120 mm
Connecting Rod Length	192 mm
Geometric Compression Ratio	14:1
No. of Valves	4
IVO	0° CA*
IVC	202° CA*
EVO	482° CA*
EVC	8° CA*
Swirl Ratio	0.9
Fueling system	Fully Premixed
Engine Speed	1200 rpm
Intake Temperature	60 – 143°C
Intake Pressure (abs.)	100 – 240 kPa
Coolant Temperature	100°C

* 0° CA is taken to be TDC intake. The valve-event timings correspond to 0.1 mm lift.

As shown in Fig. 1b, the engine facility is equipped to use real EGR or to simulate EGR by adding N_2, CO_2 and H_2O in proportions that would result from complete combustion of the fuel (here called complete stoichiometric products or CSP). In this article, the term EGR refers only to real EGR, while the term CSP is used to refer to the simulated EGR. As shown in the figure, the EGR loop is equipped with a cooler (a gas-to-water heat exchanger), and the EGR is introduced well upstream of the intake plenum, so the EGR travels with the intake air through a series of bends before reaching the intake plenum, to insure that the intake charge is well mixed. With this configuration, the exhaust pressure must be greater than the intake pressure for EGR to flow into the intake. The required back pressure was achieved by throttling the exhaust flow using the valve shown in Fig. 1b.

Intake air was supplied by an air compressor and precisely metered by a sonic nozzle as shown in Fig. 1b. For operation without EGR, the air flow or air flow plus CSP was adjusted to achieve the desired intake pressure, as measured by a pressure transducer on the intake runner. Intake pressures varied from 100 kPa (simulating naturally aspirated conditions) to 240 kPa for the current study. All pressures given are absolute. For operation with CSP, nitrogen and carbon dioxide were supplied from gas bottles and metered with sonic nozzles. Water was supplied via a variable-speed rotary pump while the mass flow rate was determined by continuously monitoring the weight of the supply bottle on an electronic scale. The water was vaporized in the same chamber as the fuel and introduced into the intake flow near the location where the EGR is introduced as shown in Fig. 1b. For operation with EGR, the air flow was reduced from the amount required to achieve the desired intake pressure with air alone, and the valve on the EGR line was opened. The exhaust back-pressure throttle valve was then adjusted to produce enough EGR flow to reach the desired intake pressure. This typically resulted in the exhaust pressure being about 2 kPa greater than the intake pressure. For consistency, the back pressure was maintained at 2 kPa above the intake pressure, even when EGR was not used. The EGR fraction was varied by adjusting the amount of supplied air, and then adjusting the exhaust throttle to maintain the desired intake pressure.

To achieve partial fuel stratification, a combination of premixed and DI fueling was used. The premixed fueling system, shown at the top of the schematic in Fig. 1b, consists of a GDI injector

mounted in an electrically heated fuel-vaporizing chamber and appropriate plumbing to ensure thorough premixing with the air and EGR upstream of the intake plenum. The DI fueling is accomplished using a second GDI injector mounted centrally in the cylinder head. A positive displacement fuel flow meter was used to determine the amount of fuel supplied. The fuel was a research-grade gasoline supplied by Chevron-Phillips Chemical Co., and its specifications are listed in Table 2. Note that this fuel meets the same basic specifications as the fuel used in our previous study of boosted HCCI [9], but it is from a different batch, and there are small difference in composition and the distillation curve.

TABLE 2. Chevron-Phillips Research-Grade Gasoline*

Antiknock Index (R+M)/2	87.6
RON	91.7
MON	83.4
Specific gravity	0.753
Carbon, wt%	86.27
Hydrogen, wt%	13.73
Oxygen, wt%	<0.05
A/F Stoichiometric	14.62
Lower Heating Value, gas-phase fuel (MJ/kg)	42.94
LHV for stoichiometric charge (MJ/kg)	2.749
Hydrocarbon Type, vol%	
Aromatics	25.7
Olefins	5.0
Saturates	69.3
Distillation, °C	
5%	56
10%	63
30%	81
50%	101
70%	118
90%	147
95%	161

* Based on analysis provided by Chevron-Phillips.

Similar to some of our other recent works [13,14], this work uses an equivalence ratio based on total charge mass, rather than air alone. This equivalence ratio, referred to as the charge-mass equivalence ratio (ϕ_m), is defined as $\phi_m = \dfrac{(F/C)}{(F/A)_{stoich}}$, where *F/C* is the mass ratio of fuel and total inducted charge gas (*i.e.* fresh air and EGR), and $(F/A)_{stoich}$ is the mass ratio of stoichiometric fuel/air mixture for complete combustion. This provides a convenient and consistent way to compare data with the same supplied energy content per unit charge mass (*i.e.*, the same dilution level) for operating conditions with different fuels and different EGR levels. Note that ϕ_m is the same as conventional air-based ϕ when no EGR is used. It should also be noted that the air-based ϕ is < 1 for all conditions presented, so combustion is never oxygen limited.

Prior to starting the experiments, the engine was fully preheated to 100°C by means of electrical heaters on the "cooling" water and lubricating-oil circulation systems. In addition, the intake tank and plumbing were preheated to 50 - 60°C to avoid condensation of the fuel or water from the EGR gases. An auxiliary heater mounted close to the engine provided precise control of the intake

temperature to maintain the desired combustion phasing. Intake temperatures ranged from 60° - 143°C. All data were taken at an engine speed of 1200 rpm.

DATA ACQUISITION

Cylinder pressure measurements were made with a transducer (AVL QC33C) mounted in the cylinder head approximately 42 mm off center. The pressure transducer signals were digitized and recorded at ¼° CA increments for one hundred consecutive cycles. The cylinder-pressure transducer was pegged to the intake pressure near bottom dead center (BDC) where the cylinder pressure reading was virtually constant for several degrees. Intake temperatures were monitored using thermocouples mounted in the two intake runners close to the cylinder head. Firedeck temperatures were monitored with a thermocouple embedded in the cylinder head so that its junction was about 44 mm off the cylinder center and 2.5 mm beneath the surface. Surface temperatures were estimated by extrapolating the thermocouple reading to the surface, using the thickness of the firedeck and assuming that its back surface was at the 100°C cooling-water temperature [13]. For all data presented, 0° crank angle (CA) is defined as TDC intake (so TDC compression is at 360°). This eliminates the need to use negative crank angles or combined bTDC, aTDC notation.

The crank angle of the 50% burn point (CA50) was used to monitor the combustion phasing, and the 10% burn point (CA10) was used as a representative marker for the hot-ignition point. CA10 and CA50 were determined from the cumulative apparent heat-release rate (AHRR), computed from the cylinder-pressure data (after applying a 2.5 kHz low-pass filter [12]). Computations were performed for each individual cycle, disregarding heat transfer and assuming a constant ratio of specific heats [19]. The average of 100 consecutive individual-cycle CA10 or CA50 values were then used to monitor CA10 or CA50 during operation and for the values reported. The reported PRRs and ringing intensities are computed from the same low-pass-filtered pressure data. For each cycle, the maximum PRR was analyzed separately with a linear fit over a moving ±0.5° CA window. Similar to CA50, these individual-cycle values were then averaged over the 100-cycle data set.

The acceptable knock limit for HCCI engines is often defined in terms of a maximum allowable PRR ($dP/d\theta$, where θ is a variable representing °CA). However, this does not correctly reflect the potential for knock under boosted conditions where the cylinder pressure changes significantly. In this work, the correlation for ringing intensity developed by Eng [20] is used as a measure of engine knock.

$$\text{Ringing Intensity} \approx \frac{1}{2\gamma} \cdot \frac{\left(0.05 \cdot \left(\frac{dP}{dt}\right)_{\max}\right)^2}{P_{\max}} \cdot \sqrt{\gamma R T_{\max}} \quad (1)$$

Where $(dP/dt)_{max}$, P_{max}, and T_{max} are the maximum values of PRR (in real time), pressure, and temperature, respectively, γ is the ratio of specific heats (c_p/c_v), and R is the gas constant. The ringing is a measure of the acoustic energy of the resonating pressure wave that creates the sharp sound commonly known as engine knock. Based on the onset of an audible knocking sound and the appearance of obvious ripples on the pressure trace, a ringing criterion of 5 MW/m^2 was selected as the ringing limit for operation without knock. This corresponds to about 8 bar/°CA at 1200 rpm, naturally aspirated. It should be noted that as P_{in} is increased above 100 kPa, $dP/d\theta$ can exceed 8

bar/°CA since the corresponding increased value of P_{max} in the denominator of Eq. 1 reduces the ringing intensity for a given PRR. At all boost levels tested, perceived engine knock correlated well with the ringing intensity rising above 5 MW/m^2, giving confidence in this correlation.

A second method of computing the HRR was used for detailed HRR-curve analysis of the effects of PFS presented in the second part of the results. Here, the heat release was computed in a more refined way from the ensemble-averaged pressure trace (with the 2.5 kHz low-pass filter applied), using the Woschni correlation for heat transfer [19]. Using the ensemble-averaged pressure trace has benefits from the standpoint of reduced noise on the heat-release traces. On the other hand, it can lead to overestimated burn durations if the cycle-to-cycle variations are large. However, for the condition where this was applied, the phasing was fairly stable with the standard deviation of CA50 over 100 fired cycles averaging about 1.2° CA. Moreover, the results of this detailed HRR analysis are mainly used for comparisons of the early part of the heat release, leading up to hot ignition. Since these early autoignition reactions persist for 15° - 25° CA, the relatively small cycle-to-cycle variation in CA50 will have little effect.

Exhaust emissions data were also acquired, with the sample being drawn from the exhaust plenum using a heated sample line (see Fig. 1b). CO, CO_2, HC, NOx, and O_2 levels were measured using standard exhaust-gas analysis equipment. In addition, a second CO_2 meter monitored the intake gases just prior to induction into the engine. This allowed the EGR fraction of the intake gases to be computed from the ratio of the intake and exhaust CO_2 concentrations. Smoke measurements were also made with an automated smoke meter.

RESULTS AND DISCUSSION

Φ–SENSITIVITY OF GASOLINE

As discussed in the introduction, the successful application of partial fuel stratification to reduce the HRR requires that the autoignition timing be sensitive to variations in the local ϕ. To determine the ϕ-sensitivity, the change in fuel-chemistry effects on autoignition must be isolated from the change in thermal effects (wall and residual-gas temperatures) and the effects of residual-gas composition as the global ϕ is varied. To accomplish this, an alternate-firing method is used, as in [10,11,14], where 19 cycles fire at a baseline ϕ, followed by 1 cycle fired at the ϕ of interest, for which the data are acquired. In this manner, the wall temperature remains nearly constant as the ϕ of cycle 20 is varied, since heating is dominated by the 19 cycles whose ϕ remains constant [11]. Additionally, the temperature and composition of the residuals in the charge of cycle 20 remain constant since they always come from the 19th cycle fueled at the same baseline ϕ.

Changing the fueling rate from cycle to cycle for this alternate-firing technique, requires the use of direct fuel injection. However, DI fueling can potentially change the in-cylinder thermal conditions and mixture homogeneity, even for early injection [21]. To minimize this, most of fuel is supplied with the premixed fueling system, and only a small portion is directly injected to reach the required ϕ. For example, for a baseline ϕ of 0.42, 80% of the baseline fuel (corresponding to ϕ = 0.34) is premixed. DI is then used to add ϕ = 0.08 to reach the baseline ϕ. For a test with ϕ < 0.42, the DI ϕ of cycle 20 is reduced below 0.08, while the premixed fueling remains constant. Similarly, for a test ϕ > 0.42, the DI ϕ of cycle 20 is increased above 0.08. Note that the test ϕ can not be lower than 0.34 in this case. Also, in order to generate as homogeneous of a mixture as possible, an early DI timing, 40°CA, is used. This timing was determined from a preliminary DI timing sweep at a

base ϕ to ensure good mixture homogeneity and no piston wetting by comparing the performance with the fully premixed case.

To determine the ϕ-sensitivity, CA10 of the base-ϕ condition (*i.e.* all 20 cycles fired at the baseline ϕ) is first adjusted to a selected value (368° CA for the data in Fig. 2a) by adjusting T_{in} and the amount of CSP (simulated EGR) supplied. These values are then held constant while the ϕ of cycle 20 is varied above and below the baseline ϕ value, and the change in CA10 is recorded (ensemble averaged over 20 ϕ-of-interest cycles).

Figure 2a shows the ϕ-sensitivity at P_{in} = 1 bar (naturally aspirated) of gasoline, compared to previous data at this same intake pressure for PRF73 and iso-octane from Ref. [13]. At these conditions, PRF73 is a two-stage-ignition fuel, while gasoline and iso-octane are single-stage ignition fuels. The ϕ-sensitivity is shown in terms of CA10, which is indicative of the hot-ignition timing. PRF73 shows significant advancement of CA10 with increasing ϕ as result of the strong dependence of its robust pre-ignition reactions (reactions responsible for the LTHR and ITHR) on the fuel concentration. Thus, PRF73 is quite ϕ-sensitive, and a range of autoignition times can be expected from an in-cylinder ϕ distribution produced by PFS, with a commensurate reduction in the HRR as shown in [13]. In contrast, CA10 for gasoline (P_{in} = 1 bar) is moderately retarded with increasing ϕ. This behavior is similar to iso-octane, which has autoignition characteristics similar to gasoline at these conditions [22]. Both of these fuels have relatively weak pre-ignition reactions that are not sensitive to changes in fuel concentration. As a result, their CA10 behavior is dominated by the decrease in γ (c_p/c_v) with increased fueling, which reduces the compressed-gas temperature, causing CA10 to become retarded. Gasoline is retarded slightly less than iso-octane, indicating that its pre-ignition chemistry is slightly enhanced by increasing ϕ, but not enough to overcome the γ effect. Note that this same cooling effect also occurs for PRF73, but its ϕ-sensitivity is sufficiently strong to overcome it and still advance CA10 significantly. These findings are in good agreement with a comparison of the ϕ-sensitivity of gasoline, iso-octane, and PRF80 at a similar operating condition [11]. This lack of ϕ-sensitivity for gasoline at P_{in} = 1 bar suggests that PFS will not be effective for reducing the HRR for naturally aspirated operation.

However, intake pressure boosting significantly enhances the autoignition reactivity of gasoline as discussed in the Introduction, and in greater depth in Ref. [9]. As shown in our previous work [9], the ITHR increases substantially as boost levels are increased from 1 to 2 bar. To prevent this enhancement from causing overly advanced combustion timing, T_{in} was decreased from around 140°C to 60°C and significant amounts of EGR were added. The 60°C low-temperature limit was chosen to prevent water condensation in the cooled EGR gases. With T_{in} = 60°C significant LTHR was not observed. Only a small hint of LTHR could be seen on a highly amplified scale for P_{in} of 1.8 bar and higher. Thus, gasoline remained largely a single-stage fuel over the boost range studied in [9], 1 - 3.25 bar. Despite this single-stage behavior, the large increase in pre-ignition reactivity in terms of increased ITHR, suggests that gasoline may become ϕ-sensitive under boosted operation.

To test this hypothesis, ϕ-sensitivity sweeps were conducted for P_{in} = 2 and 1.6 bar. Because the pressure rise with combustion is greater for boosted operation, more timing retard is required to prevent excessive ringing (knock). Therefore, it was not possible to match both the base ϕ = 0.42 and CA10 of the naturally aspirated data in Fig. 2a. Accordingly, two ϕ-sensitivity sweeps were conducted for P_{in} = 2 bar: one matching the base-ϕ = 0.42 in Fig. 2a but with CA10 retarded about 5° CA, and another matching the CA10 = 368° CA in Fig. 2a, but with a base-ϕ = 0.345. A ϕ-

sensitivity sweep was also conducted for P_{in} = 1.6 bar matching the CA10 in Fig. 2a with a base-ϕ = 0.367.

Figure 2b presents the results of these boosted gasoline sweeps along with the P_{in} = 1 bar gasoline and PRF73 data from Fig. 2a. As can be seen, gasoline has a very strong ϕ-sensitivity at P_{in} = 2 bar for both ϕ ranges, and a moderate ϕ-sensitivity at P_{in} = 1.6 bar. In fact, the ϕ-sensitivity of gasoline at P_{in} = 2 bar is even stronger than that of PRF73 as evident by its steeper slope in Fig. 2b. At P_{in} = 1.6 bar, the sensitivity is somewhat less than PRF73, but still significant. These results suggest that PFS should be effective for reducing the HRR of boosted HCCI which could allow higher fueling rates without excessive ringing (knock) and/or more advanced combustion phasing for higher efficiency. Additionally, they suggest that the ITHR pre-ignition reactions are as important, or perhaps more important, for determining ϕ-sensitivity than the LTHR reactions previously thought to be key [10,11,13].[3]

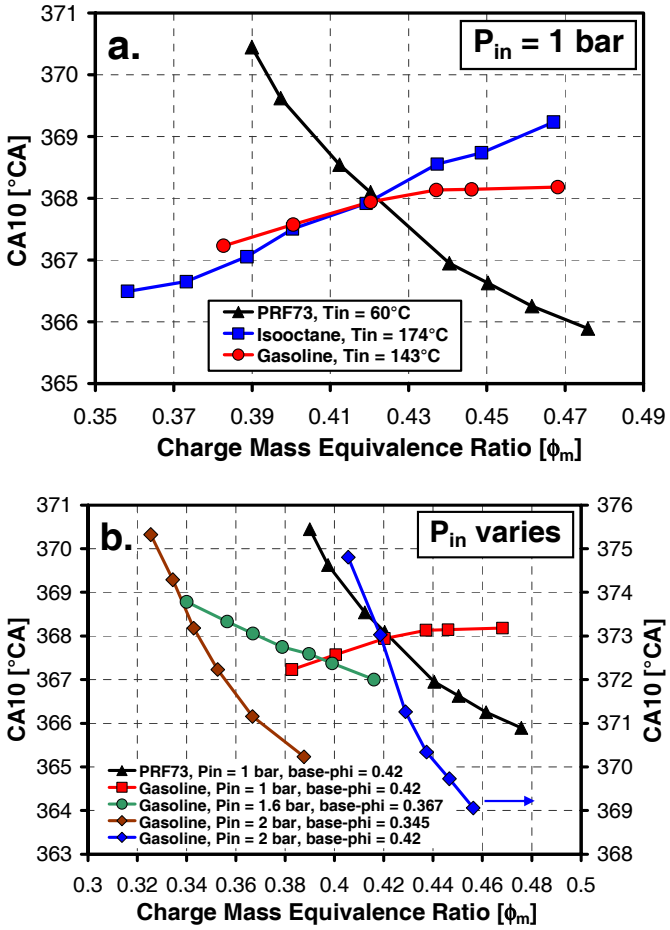

Figure 2. ϕ-sensitivity of gasoline compared to PRF73 and iso-octane from Ref. [13] (a) at P_{in} = 1 bar, and (b) for gasoline P_{in} = 1, 1.6 and 2 bar. For Fig. 2a, the base-ϕ = 0.42 for all fuels and T_{in} = 60°C, 174°C, and 143°C for PRF73, iso-octane, and gasoline, respectively. Fig. 2b repeats the gasoline and PRF73 data from Fig. 2a, and also includes gasoline at P_{in} = 1.6 bar, base-ϕ = 0.367, T_{in} = 93°C, and gasoline at P_{in} = 2 bar and T_{in} = 60°C for two fueling ranges: base-ϕ = 0.42 and base-ϕ = 0.345.

[3] In a concurrent work [14], the authors also conclude that ITHR is quite important for ϕ-sensitivity, based on other comparisons between fuels.

PARTIAL FUEL STRATIFICATION OF GASOLINE

The ϕ-sensitivity results for gasoline in Fig. 2 indicate that partial fuel stratification should be effective for reducing the HRR in HCCI engines when the intake pressure is boosted above about 1.6 bar, but not for naturally aspirated conditions. To verify this, experiments were conducted with intake pressures of 1 and 2 bar to determine the effects of PFS on the HRR using various fueling strategies. As discussed in the introduction, PFS involves premixing most of the fuel, while the remainder is directly injected in the latter part of the compression stroke. With this technique, the amount of mixture stratification (*i.e.* the mass-weighted ϕ_m-distribution of the charge) depends on both the DI timing and the fraction of the total fuel delivered by DI injection. Previous works have shown that the amount of stratification and commensurate HRR reduction can be increased by either shifting the DI timing later in the compression stroke for a fixed DI fraction or by increasing the DI fraction for a fixed DI timing [10,13,14]. All DI timings given correspond to the start of injection.

In the current study, a DI-timing sweep is conducted followed by a DI fraction sweep for both intake pressures, 1 and 2 bar. Since changes in combustion phasing can affect the HRR and PRR independent of any effect of PFS, CA50 was held constant for each sweep by varying the amount of CSP (*i.e.* some of the excess air is replaced with CSP). Using variable CSP to control CA50, rather than varying T_{in}, keeps the intake density constant, so the total mass flow through the engine and the global ϕ_m remain constant during the sweep.

Partial Fuel Stratification for P_{in} = 1 bar

Figure 3 shows the effect of varying the DI timing for a relatively high HCCI load, corresponding to a global ϕ_m = 0.44, for P_{in} = 1 bar. For this sweep, the DI fraction was held constant at 6% (by mass), and CA50 was held at 371° CA. Before introducing any stratification, engine operation was stabilized at the desired CA50 with fully premixed fueling by setting T_{in} = 143°C with the air diluted by 5.2% CSP. This operating point is shown as an injection timing of 0° CA in Fig. 3. Then, the fueling was switched to PFS (94% premixed and 6% DI) and data were acquired for DI timings from 280 - 335° CA. As can be seen, for gasoline PFS with P_{in} = 1 bar, increasing the stratification with delayed DI timing has almost no effect on the maximum PRR or ringing intensity (derived from the PRR using Eq. 1).

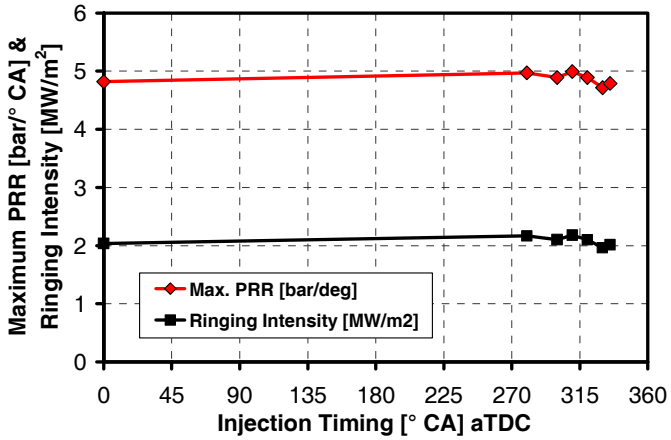

Figure 3. The effect of varying DI timing with a constant DI fraction of 6% on the ringing intensity and maximum PRR for gasoline at P_{in} = 1, ϕ_m = 0.44, T_{in} = 143°C.

Similarly, increasing the stratification by increasing the DI fraction for a constant DI timing of 310° CA also has no benefit for reducing the maximum PRR or ringing intensity with P_{in} = 1 bar. Note that the fully premixed base condition for this DI fraction sweep is the same as for the DI timing sweep (ϕ_m = 0.44, CA50 = 371° CA, T_{in} = 143°C, 5.2% CSP). Figure 4 shows the results of this sweep with gasoline together with those for a similar sweep with iso-octane from Ref. [13]. As can be seen, both fuels show very similar trends, with ringing or PRR actually increasing slightly with increased DI fraction. These results confirm that mixture stratification does not produce a staged combustion process for either of these two fuels at this P_{in}, or it is so weak that it is dominated by other processes. The lack of any reduction in the ringing for either the DI timing or DI fraction sweeps is in agreement with the lack of significant ϕ-sensitivity as shown in Fig. 2.

The cause of this slight increase in ringing with DI fraction is not known. As discussed in [13] with respect to the iso-octane data, one possibility is that the spray-induced mixing and/or vaporization, resulting from the DI injection, alter the naturally occurring thermal stratification [23,24]. If the fuel injection process removed some of the hottest zones that would have ignited first, it could produce a more thermally uniform charge resulting in more rapid combustion. This explanation is supported by the PRR and HRR data in Fig. 5, which show a slight delay in the onset of hot ignition and a shorter burn duration with a higher peak HRR as the DI fraction increases. However, these trends are small in any event, and the main conclusion from Fig. 5 is that PFS hardly changes the HRR or PRR for gasoline at P_{in} = 1 bar.

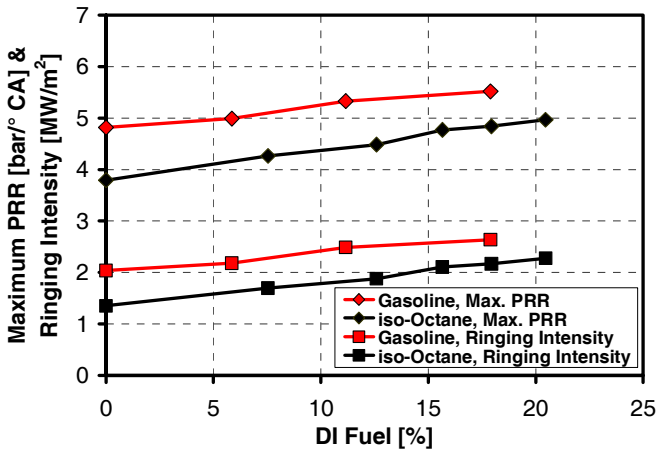

Figure 4. The effect of varying DI fraction with a constant DI timing of 310° CA. on the ringing intensity and maximum PRR for gasoline at T_{in} = 143°C and iso-octane at T_{in} = 174°C from Ref. [13]. All other parameters are the same for both fuels: P_{in} = 1, ϕ_m = 0.44, and CA50 = 371° CA.

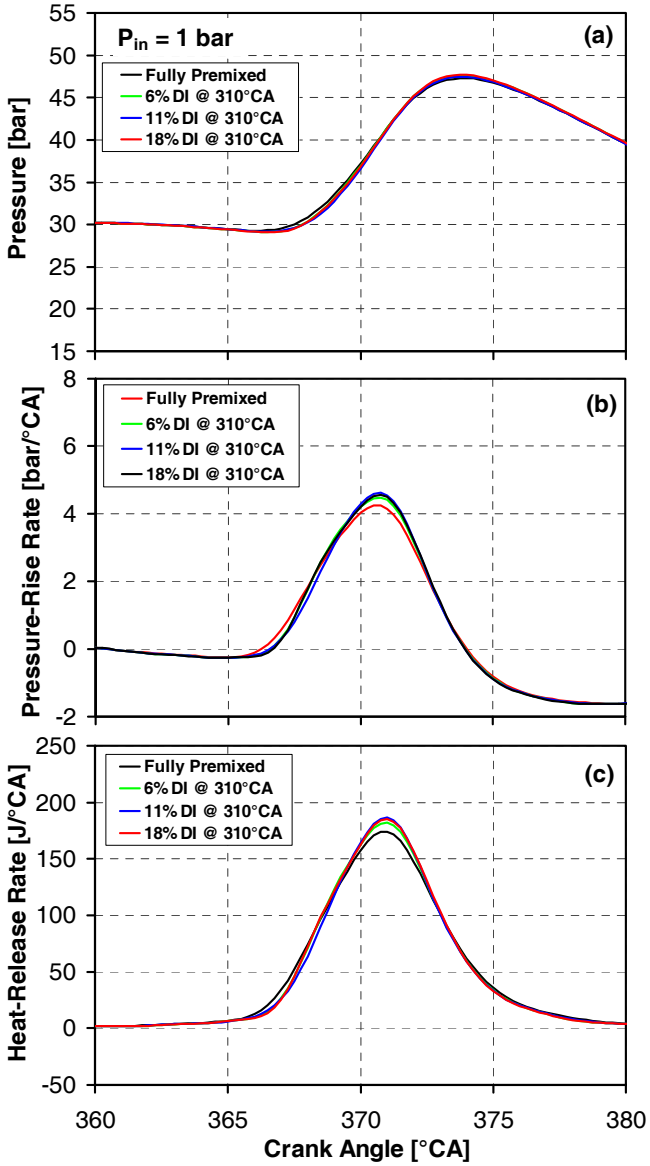

Figure 5. The effect of varying DI fraction for P_{in} = 1 bar: (a) cylinder pressure, (b) PRR, and (c) HRR, corresponding to the gasoline data points presented in Fig. 4.

Partial Fuel Stratification for P_{in} = 2 bar

In sharp contrast with the results at P_{in} = 1 bar, PFS is found to be quite effective for reducing the PRR and ringing intensity for P_{in} = 2 bar. Figure 6 show the results of increasing the mixture stratification by retarding the DI timing with a constant DI fraction of 13%. Similar to the P_{in} = 1 bar sweeps presented above, the engine was first stabilized with fully premixed fueling with ϕ_m = 0.44, but CA50 was retarded to 377° CA to prevent excessive ringing, $IMEP_g$ = 11.1 bar. Note that the ringing intensity of 6.1 MW/m^2 for this baseline point is a little above the no-knock limit of 5 MW/m^2. Also, since gasoline is much more reactive with intake boost, T_{in} was reduced to 60°C and the CSP increased to 26.7% for this baseline premixed point.

Fueling was then switched to PFS with 13% DI, and the injection timing was progressively retarded to increase the fuel stratification. T_{in} was held constant at 60°C, and the amount of CSP was adjusted to maintain CA50 = 377° CA. As can be seen (Fig. 6), ringing increases slightly above the

premixed point for a DI timing of 100° CA, then it drops rapidly as the stratification becomes significant for DI timings ≥ 200° CA. This indicates that the ϕ-distribution produced by these later DI timings, combined with the strong ϕ-sensitivity of gasoline at P_{in} = 2 bar (Fig. 2b), results in a staged combustion process with the richest regions autoigniting first followed by the next richest and so on. Also, because these richer regions autoignite faster, PFS tends to advance the combustion phasing. To compensate, the amount of CSP was increased to maintain a constant CA50 as the amount of stratification increased. Figure 7 shows the reduction in intake oxygen resulting from the increased CSP.

By the time injection is retarded to 285° CA, PFS has reduced the ringing from 6.1 to 2.1 MW/m^2. This corresponds to such a low burn rate that any further reduction results in significant combustion instability. Therefore, CA50 was advanced to 374° CA as indicated in legend of Fig. 6, and data were acquired for DI timings of 285 – 305° CA. As evident in the figure, this advancement of CA50 at DI-timing = 285° CA increases the ringing to nearly 7. However, further increasing the stratification by retarding the DI timing from 285 – 305° CA reduces the ringing again to less than 2. To explore the effects of further stratification, CA50 was then advanced to 372.3° CA and the DI timing retarded to 320° CA, bringing the ringing back to about 2 MW/m^2. As shown in Fig. 7, these advancements in CA50 were accomplished by decreasing the CSP at a given DI timing. Then, at the new timing CSP was increased again to maintain CA50 as the DI timing was further retarded.

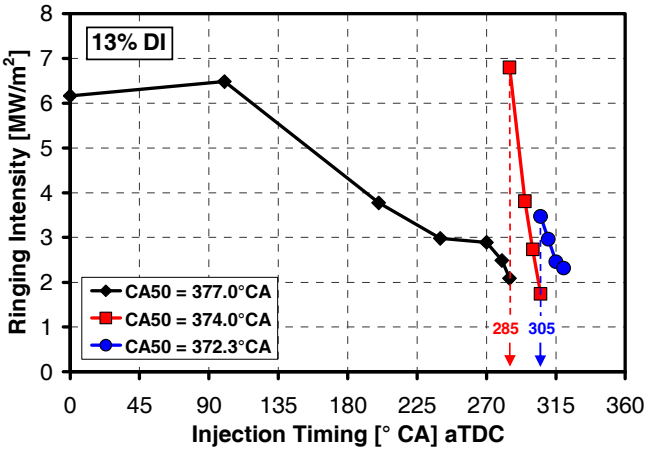

Figure 6. The effect of varying DI timing with a constant DI fraction of 13% on the ringing intensity for gasoline at P_{in} = 2, ϕ_m = 0.44, T_{in} = 60°C.

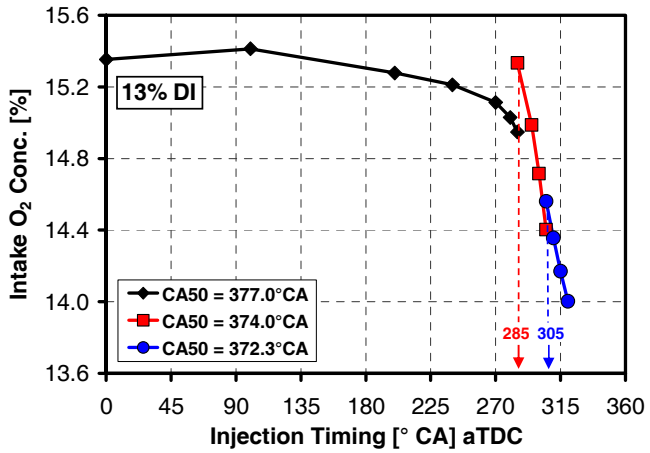

Figure 7. Intake oxygen concentration as a measure of CSP for the DI timing sweeps in Fig. 6 (gasoline at P_{in} = 2, ϕ_m = 0.44, T_{in} = 60°C, CSP = 26.7 – 33.1%).

As discussed previously, the amount of PFS can also be increased by increasing the DI fraction. Figure 8 shows that a substantial reduction in ringing intensity can be achieved by increasing the DI fraction from 3 – 20% for a constant DI timing of 300° CA at a constant CA50 = 374° CA. A fully premixed point was not included in this sweep because the ringing would reach unsafe levels with this CA50 = 374° CA combustion phasing. Note that the ringing is already at 10 MW/m^2 for a DI fraction of 3% (double the 5 MW/m^2 value for the onset of knock). Maintaining a constant CA50 as the stratification increased with increasing DI fraction required an increase in CSP as shown by the reduced intake oxygen concentration plotted at the top of Fig. 8.

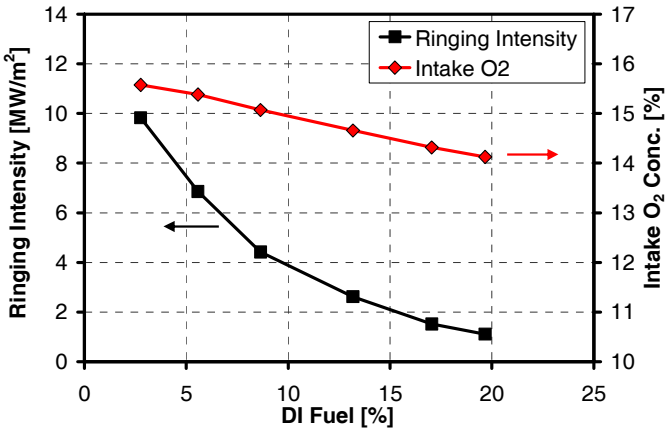

Figure 8. Ringing intensity and intake oxygen concentration (a measure of CSP) for variations in DI fraction with a constant DI timing of 300° CA (gasoline at P_{in} = 2, ϕ_m = 0.44, T_{in} = 60°C, CSP = 25.6 – 32.7%).

The corresponding cylinder-pressure, PRR, and HRR traces in Fig. 9 show that increasing the DI fraction over this range has a substantial impact on the combustion event. With increasing DI fraction, the increased regions of higher ϕ_m autoignite sooner, advancing the onset of hot ignition for the same CA50, as evident in all three plots in Fig. 9. This effectively increases the burn duration as can be seen in Fig. 9c, and it reduces the peak HRR and maximum PRR in agreement with the reduction in ringing intensity shown in Fig. 8. The peak cylinder pressure is also reduced (Fig. 9a). Finally, it should be noted that the data in Fig. 9 start with a DI fraction of 3%, which is already significantly smoothed by PFS. If the fully premixed case could have been run, the change in the cylinder-pressure, PRR, and HRR traces would appear even more dramatic.

The results in Figs. 6 – 9 show that PFS is very effective for extending the HCCI combustion duration and reducing the maximum PRR for gasoline fueling at an intake pressure of 2 bar. As shown in Fig. 6, this can allow a significant advancement of the combustion phasing for the same overall fueling rate, resulting in the thermal efficiency increasing by about 1 percentage unit. The $IMEP_g$ also increased with PFS up to 11.3 bar compared to 11.1 bar for fully premixed fueling. Moreover, all the other combustion, efficiency, and emissions parameters remain comparable or better than the those of the fully premixed baseline point shown in Figs. 6 and 7 (*i.e.* the point plotted as 0° CA). For all the PFS data presented in this section, the COV of $IMEP_g$ never exceeded 2.4% and is typically well under 2%. Combustion efficiency ranges from 96.8 – 97.8%, and the indicated gross thermal efficiency ranges from 44.1 – 45.3%. NOx emissions are more than an order of magnitude below the US-2010 limit for all cases except for the very late DI timings used for the CA50 = 372.3° CA cases in Figs. 6 and 7, and even the worst case is still a factor of 2 below the US-2010 limit. Finally, the highest soot emissions measured were more than an order of magnitude below the US 2010 limit, and for most cases they were near or below the detection limit

of our smoke meter. A complete series for plots of these parameters for the DI-timing and DI-fraction sweeps is provided in the Appendix.

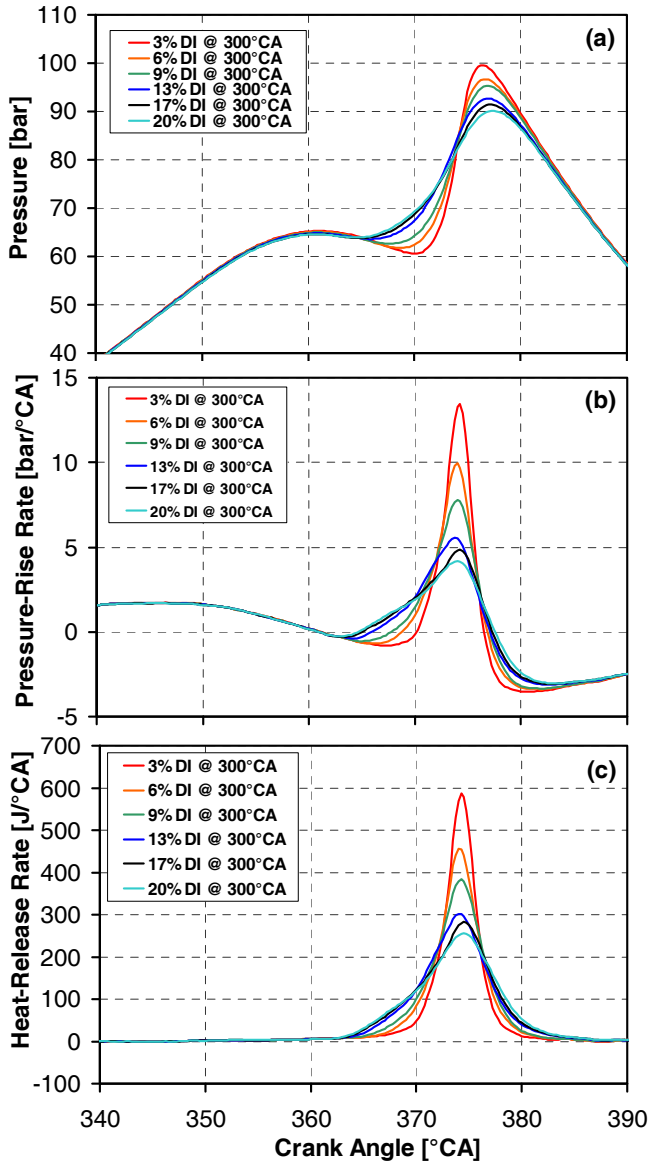

Figure 9. The effect of varying DI fraction at a constant DI-timing = 300° CA for P_{in} = 2 bar: (a) cylinder pressure, (b) PRR, and (c) HRR, corresponding to the data points presented in Fig. 8.

EXTENDING THE HIGH-LOAD LIMIT WITH PFS

Increasing ϕ_m to the High-Load Limit for P_{in} = 2 bar

With its demonstrated effectiveness for reducing the ringing intensity and allowing more advanced combustion phasing, PFS has a strong potential for extending the high-load limit of HCCI under boosted operation. To investigate this potential, a study was conducted to determine the high-load limit at P_{in} = 2 bar for PFS compared to fully premixed fueling. Data were also acquired for 100% DI fueling during the intake stroke, with a start-of-injection timing of 80° CA. For the fully

premixed and full DI strategies the fueling rate was increased from $\phi_m = 0.3$ up to the knock/stability limit [9].[4] The sweep for PFS also extends to the knock/stability limit, but it starts at $\phi_m = 0.36$ since PFS has no significant advantage at fueling rates as low as $\phi_m = 0.3$. Combustion phasing was controlled by the addition of real EGR, rather than CSP, and the intake temperature was held constant at 60°C.

Figure 10 shows the increase in $IMEP_g$ for the three strategies along with the COV of the $IMEP_g$. For fully premixed fueling, the maximum load is $IMEP_g = 11.7$ bar at $\phi_m = 0.47$. This slightly higher than the maximum $IMEP_g = 11.5$ bar reported in Ref. [9] for this boost level. The difference is attributed to a different batch of gasoline that was slightly more stable at this high-load point. Full DI fueling yielded the lowest maximum $IMEP_g = 10.7$ bar at $\phi_m = 0.40$, which was somewhat surprising since this fueling method does produce some mixture stratification even with this early injection timing, as shown in a recent optical imaging study in this engine [21]. However, combustion became very unstable leading to runaway knock at higher fueling rates. The reason is unclear, perhaps there were large variations in mixture stratification in the outer part of the combustion chamber (*i.e.* near the cylinder wall) that were not visible in the imaging study [21]. Switching to PFS completely eliminated the problem at these fueling rates ($\phi_m = 0.40$) and allowed much higher loads.

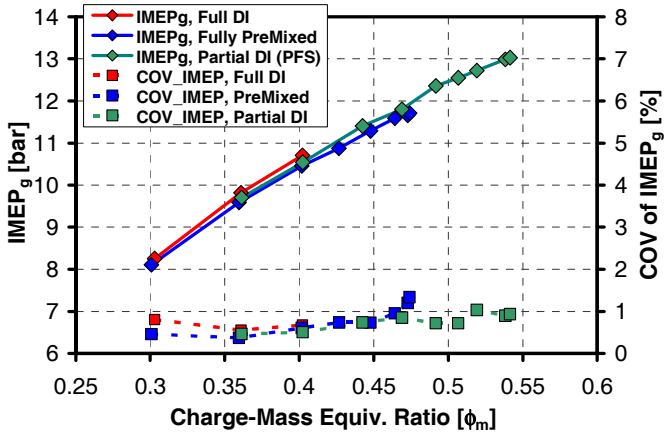

Figure 10. $IMEP_g$ and COV of $IMEP_g$ for three fueling strategies: full DI, PFS (partial DI), and fully premixed for a range of fueling rates up to the high-load limit for each case.

As with the results in the previous subsection, PFS substantially reduced the ringing compared to premixed fueling. This allowed less CA50 retard for loads near the premixed high-load limit. It also made the combustion more robust at these fueling rates. As a result, fueling could be increased significantly as shown in Fig. 10. Based on the study in the previous section of the effects of variations in DI timing and DI fraction on the performance with PFS, 10% DI at 310° CA was selected for the start of the ϕ-sweep shown in Fig. 10. However, as the load increased above about $IMEP_g = 12$ bar, the combustion began to become unstable with this setting, and better performance was obtained with 7% DI at a timing of 315° CA. This latter setting was used for the remainder of the sweep. Another key factor for high-load operation with PFS at $P_{in} = 2$ bar is that if CA50 was advanced to the ringing limit of 5 MW/m^2, the combustion tended to go to runaway knock.

---

[4] As fueling is increased the combustion phasing must be retarded to control knock, but too much retard causes the combustion to become unstable. Eventually, a point is reached beyond which the fueling cannot be increased without leading to runaway knock or the combustion becoming very unstable and misfiring. This knock/stability limit is discussed in more detail in Ref. [9].

However, if the ringing was kept to the 2 – 3 MW/m^2 range, it was much more stable, and higher loads could be achieved. Using this strategy, the load was extended to IMEP$_g$ = 13.0 bar at ϕ_m = 0.54. This is a very high fueling rate for HCCI-like combustion and a very high load for P_{in} = 2 bar. In fact, it is approaching the stoichiometric limit, with only 1% oxygen remaining in the exhaust due to the amount of EGR required to maintain combustion timing. Also, since the full range of combinations of DI timing and DI fraction have not been well explored, it may be possible to adjust the fuel stratification for greater stability and increase the load up to the oxygen-availability limit. Finally, it should be noted that for all data points presented in Fig. 10, cycle-to-cycle stability was very good with the COV of IMEP$_g$ being on the order of 1%, as plotted at the bottom of the figure.

Figure 11a shows the CA50 timings and EGR levels for all three fueling strategies. For each strategy, CA50 was retarded as load was increased to control the ringing intensity and/or to maintain stability. As can be seen, EGR levels were typically increased to achieve this increased retard, but the EGR curves tend to flatten at the higher loads as the composition of the EGR shifts to containing more combustion products and less air.

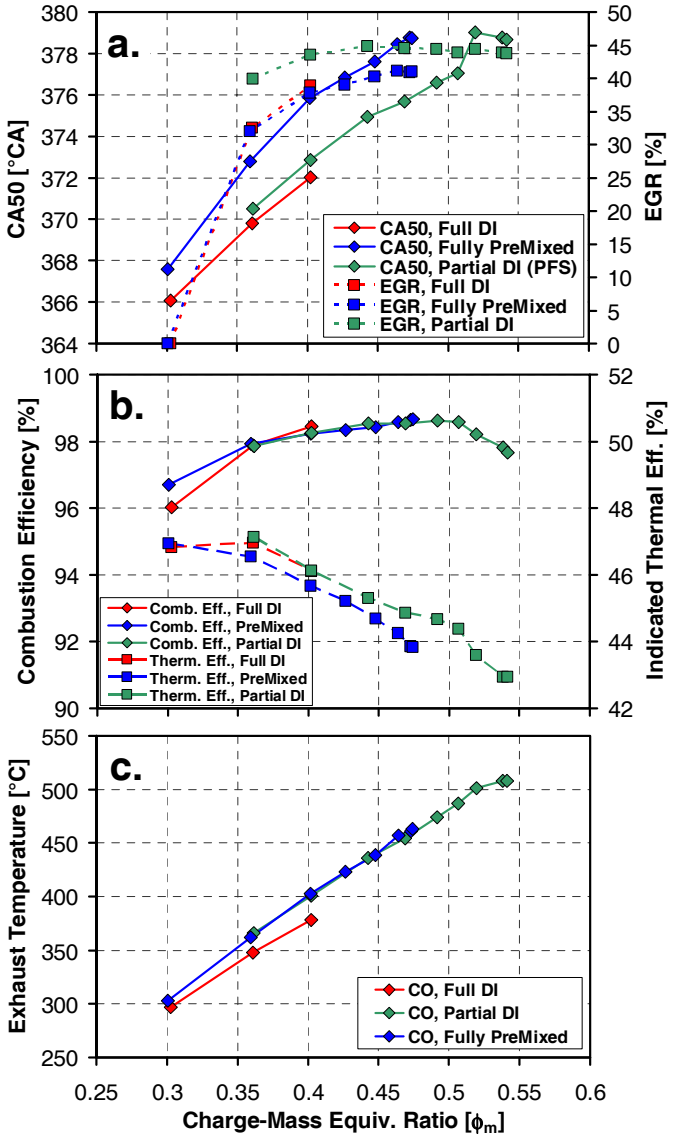

Figure 11. (a) CA50 and EGR percent, (b) combustion and thermal efficiencies, and (c) exhaust temperatures corresponding to the data in Fig. 10.

Combustion and indicated-thermal efficiencies are presented in Fig. 11b. Combustion efficiencies are very good for all the high load cases, typically above 98%. For all three strategies, the combustion efficiency increases with ϕ_m due to higher combustion temperatures that tend to better burn the cooler gases close to the wall and the gases exiting the crevices during the first part of the expansion. Also, the increased EGR levels decrease the total throughput of gases through the engine reducing the mass of CO and HC exiting the exhaust (*i.e.* a significant fraction of the CO and HC in the exhaust gets a second chance to burn) [9]. The drop in combustion efficiency at the highest loads with PFS corresponds to an increase in CO (Fig. 12a) and is thought to be due to insufficient oxygen in the richest stratified regions. Indicated thermal efficiencies decrease moderately with increased load due to the need to retard the timing and to add EGR, the latter of which reduces expansion efficiency due to the lower γ of the EGR gases [25]. Despite this reduction, the indicated thermal efficiency remains high. It should also be noted that the brake efficiency will show less decrease with increased load, since the higher exhaust enthalpies at increased ϕ_m will be more effective at driving a turbocharger, as evident from the exhaust temperatures in Fig. 11c.

Figure 12 presents the exhaust emissions corresponding to the data in Figs. 10 and 11. As shown in Fig. 12a, CO emissions decrease dramatically as ϕ_m increases from 0.3 to 0.36. Then they decrease at a lesser rate up to $\phi_m = 0.49$ as combustion temperatures increase and EGR levels rise. As discussed above, the increase in CO for PFS at $0.49 < \phi_m < 0.54$ is thought to be due to a lack of oxygen in the richest stratified areas. Despite this increase in CO, the combustion efficiency is still very good (Fig. 11b). Similarly, emissions (Fig. 12 b) also decrease with increasing ϕ_m due to increased combustion temperatures and increased EGR. However, HC emissions do not increase for the most stratified cases since the oxygen deficit in the stratified area does not prevent the reactions from proceeding to CO and H_2O. Finally, NOx and soot (smoke) emissions remain extremely low for all points in these three sweeps.

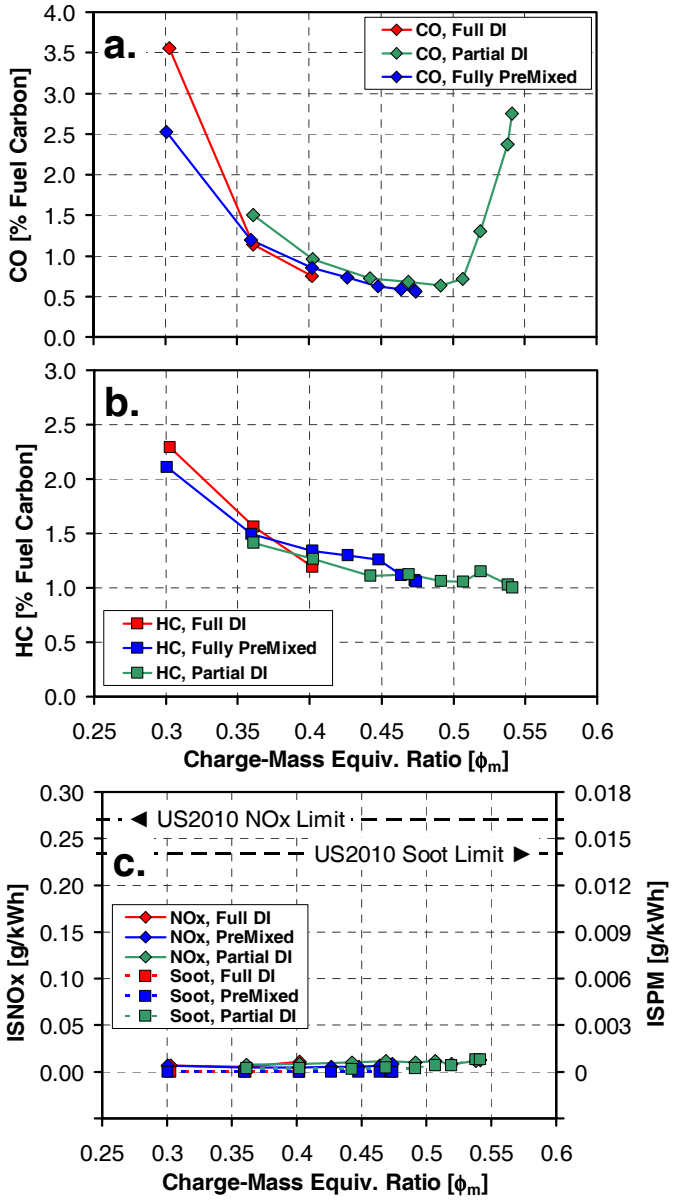

Figure 12. (a) CO, (b) HC, and (c) NOx emissions corresponding to the data in Fig. 10.

PFS vs. PM fueling – Maximum Load with Boost

The above results show that PFS works very well to extend the high-load limit of HCCI at P_{in} = 2 bar. This section explores the use of PFS for extending the high-load limit over a range of boost pressures. Examining and extrapolating the ϕ-sensitivity trends in Fig. 2b suggests that PFS is not likely work effectively much below P_{in} = 1.6 bar, its effectiveness will increase as P_{in} is increased from 1.6 to 2 bar, and it should continue to be effective for P_{in} > 2 bar. Accordingly, PFS was applied for intake pressures from 1.6 - 2.4 bar determine its potential for extending the high-load limit. Higher boost levels were not examined since the EGR levels required for premixed operation $P_{in} \geq 2.6$ bar are such that there is essentially no excess oxygen in the exhaust, so there is no potential for increasing the fueling (ϕ_m) with PFS. Note that PFS typically requires as much EGR or more than premixed to prevent CA50 advancement as discussed above (see also Fig. 11a).

Figure 13 shows the maximum load ($IMEP_g$) achieved with PFS compared to premixed fueling. Two premixed fueling lines are shown. The lower premixed curve shows the maximum load from our previous work [9], designated by its SAE paper number, SAE 2010-01-1086. Somewhat higher loads were obtained for our premixed control points in the current study, as shown in the upper premixed curve, labeled "current data". The reason for the shift is two-fold. First, a different batch of gasoline was used whose properties gave slightly better stability near the high-load limit. This accounts for the increase in $IMEP_g$ from 11.5 to 11.7 bar at P_{in} = 2 bar (discussed above), for these data which were obtained shortly after the 55 gallon fuel drum was first opened. Second, the fuel autoignition properties changed during the course of this study (several months) due to a loss of volatiles and stratification of the fuel in the 55 gallon drum (here termed fuel ageing).[5] As a result, the discrepancy between the two premixed data sets is greater for the other intake pressures, for which the current data were acquired later in the study, when this ageing effect was more prominent. Note that the early-acquired P_{in} = 2 bar "current data" point in Fig. 13 deviates downward from the trend of the other points. Also, this point was re-tested late in the study, and it was found that the maximum load increased from the 11.7 bar value shown to 12.0 bar, which would be more "in-line" with the other data points. This suggests that reducing the other "current" premixed data points by a similar amount (~0.3 bar $IMEP_g$) might give more representative values for premixed performance with fresh fuel.

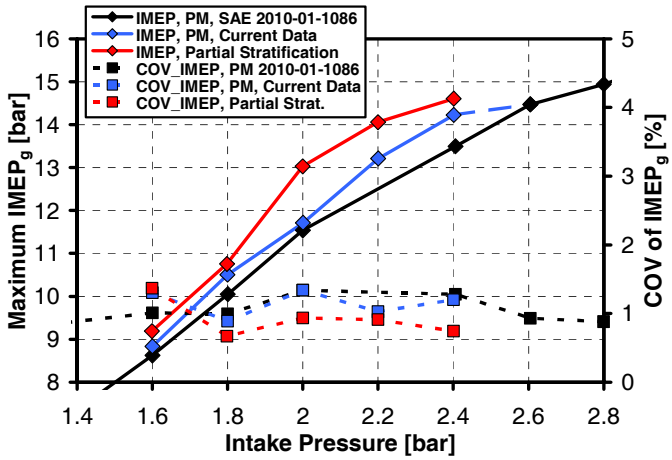

Figure 13. Maximum $IMEP_g$ attainable with premixed and PFS fueling strategies for various intake pressures. COV of $IMEP_g$ is plotted on the right-hand axis.

Nevertheless, the data in Fig. 13 show that PFS allows an increase in load for all intake pressures tested, even compared to the higher "current" premixed data points.[6] For $P_{in} \geq 2$ bar, the combustion was quite stable with PFS allowing a significantly larger load increase than for the lower intake pressures (discussed below). Although the high-load PFS point for P_{in} = 2 bar is currently limited by knock/stability, it is quite close to the oxygen-availability limit (1% oxygen remaining in the exhaust). For the higher intake pressures (2.2 and 2.4 bar), stability with PFS was even better, and the load could essentially be extended to the oxygen-availability limit, as discussed further below. In fact, at P_{in} = 2.2 and 2.4 bar, stability was very good even when CA50 was

[5] For all previous studies in our laboratory, gasoline was supplied in 5-gallon cans, and this ageing was not an issue. A procedure has been developed to prevent this behavior in future studies when fuel is supplied in 55 gallon drums.
[6] It should be noted that for each P_{in}, the PFS and premixed points were acquired in close succession (usually on the same day), so changes in fuel properties do not affect these comparisons.

advanced to allow a ringing of ~5 MW/m^2 for PFS operation, compared to P_{in} = 2 bar where a lower ringing of 2 – 3 MW/m^2 was required for good stability as discussed above.

The amount that PFS can increase the load above fully premixed fueling is somewhat uncertain due to the fuel ageing problem discussed above. The P_{in} = 2 bar data were acquired when the fuel was fresh, so they are considered the best example of high-load improvement with PFS. For P_{in}= 2.2 and 2.4 bar, the improvement compared to the current data is less than in would be if the fuel had not aged. Furthermore, the improvement compared to un-aged fuel from the current batch would still be less than the improvement compared to the premixed data from SAE 2010-01-1086. In fact, these differences illustrate the larger issue of the effect of small changes in gasoline composition, which can affect the high-load premixed limit as illustrated here. However, they are less likely to affect the high-load PFS limit which is more influenced by the ϕ-sensitivity, and for $P_{in} \geq 2.2$ bar, oxygen availability. Although ϕ-sensitivity can be affected by fuel composition, it is so strong for intake pressures in the 2 bar range (Fig. 2) that small adjustments to the mixture stratification would likely be able to compensate for any small changes due to fuel composition. Thus, it seems likely that a fuel with the composition of that used for the SAE 2010-01-1086 study could achieve essentially the same high load with PFS as shown here, particularly for the oxygen-limited cases. For these reasons, PFS potentially offers a valuable tool for maintaining the same maximum load even for small variations in gasoline composition that would otherwise affect the high-load limit for premixed operation.

Figure 14 shows exhaust oxygen and intake EGR levels corresponding to the maximum-load PFS and premixed data points in Fig. 13. As can be seen, the oxygen remaining in the exhaust drops dramatically for P_{in} > 1.6 bar for all three sweeps due to the addition of EGR, required to provide sufficient combustion-phasing retard. The oxygen levels for the PFS cases are the lowest of the three sweeps because higher EGR levels are required to control CA50 since the locally rich regions tend to autoignite faster, and because PFS allows a higher fueling rate as evident by the higher loads in Fig. 13. The difference in oxygen levels between premixed and PFS fueling becomes greater at P_{in} = 2 bar with the significant fueling (load) increase enabled by PFS. Although about 1% oxygen remains, there is potential for only a small additional increase in load with improved PFS operation since CO levels are already beginning to rise at the current high-load point (Fig. 12a). Available oxygen is even less for P_{in} = 2.2 and 2.4 bar, so these can be considered essentially at the oxygen limit.

In contrast, premixed fueling does not reach the oxygen limit until 2.6 bar for the SAE 2010-01-1086 data or 2.4 bar for the current premixed data. Note that although the PFS and current-premixed points for P_{in} = 2.4 bar have the same oxygen remaining, PFS still produces a slightly higher load (Fig. 13) because CA50 is slightly advanced, and because fueling was slightly higher. However, the increased fueling does not further reduce the oxygen, but produces a significant increase in CO (although still below acceptable limits). As evident form this example, the oxygen availability limit is not well defined, and extensive efforts to eke out bit higher load were not attempted. The small differences in the lowest oxygen levels for $P_{in} \geq 2.2$ bar are not considered significant.

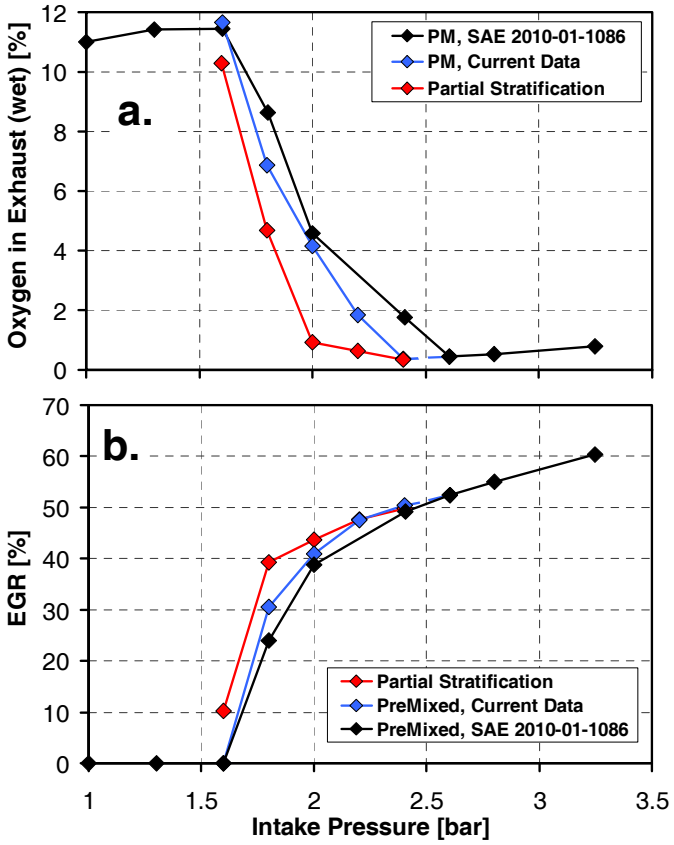

Figure 14. (a) Exhaust oxygen and (b) intake EGR mole fraction corresponding to the maximum load points presented in Fig. 13.

Because the P_{in} = 2.4 bar data points for PFS and current-premixed fueling are at the oxygen limit, higher boost pressures were not included in this study. As indicated by the dashed line, in Figs. 13 and 14, the current-premixed curve should merge with the SAE 2010-01-1086 premixed data at P_{in} = 2.6 bar, where the previous data reach the oxygen-availability limit. Exactly how the PFS line would merge is not completely clear. The maximum $IMEP_g$ for PFS at P_{in} = 2.4 bar is already slightly higher than the premixed point at P_{in} = 2.6 bar, suggesting that with its more advanced CA50, PFS could provide a bit higher load than the current premixed point at 2.6 bar if CO levels are allowed to rise as with the P_{in} = 2.4 bar point.

Although PFS allowed a significant increase in $IMEP_g$ for $P_{in} \geq 2$ bar, only a small increase could be obtained for P_{in} = 1.6 and 1.8 bar as evident in Fig. 13. For these lower P_{in}, increasing the fueling rates above the loads presented in Fig. 13 quickly led to runaway knock or misfire, even though the COV of $IMEP_g$ remains low for all data points presented (bottom plot of Fig. 13). With the hypothesis that the most likely cause was cycle-to-cycle variations in the mixture formation, several combinations of DI timing and DI fraction were tested for P_{in} = 1.8 bar. In particular, a late DI timing with a smaller DI fraction should be more dominated by jet mixing, and therefore, is expected to be more consistent from cycle to cycle than earlier injection timings, which would be more influenced in-cylinder turbulence due to the longer mixture-formation time. A late DI timing was used for the high-load P_{in} = 1.8 bar point shown in Fig. 13, but stability was only slightly better, and the load only slightly higher, than for earlier DI timings.

The onset of significant NOx formation, which can lead rapidly to runaway knock [26,27] particularly when EGR is used [28], was also considered to be a possible reason for the inability to

extend the load further with PFS at these lower P_{in}. Supporting this hypothesis, the NOx emissions corresponding to the maximum load points show slightly higher level for P_{in} = 1.8 bar (Fig. 15). Note that NOx formation is not likely to be an issue at the higher boost levels because more EGR is required to control CA50, which will also act to reduce NOx formation from the partially stratified combustion. Since NOx-induced runaway results from a few ppm of NOx in the charge, it will occur at lower loads when EGR recycles NOx rather than when CSP is used, and the only source is from the retained residuals. However, tests using CSP were not successful at extending the high-load limit, indicating that NOx-induced runaway is not likely the main cause of the current knock/stability limit. Further investigation will be required to determine the cause of the limited knock/stability limit for PFS at these lower boost levels, and to determine whether higher loads can be achieved with PFS for intake pressures in the 1.6 – 1.8 bar range.

Figure 15 shows the NOx and soot emissions for these maximum-load points. NOx emissions are extremely low for all the boosted PFS points. As mentioned with respect to the load-limit discussion above, there is a slight increase for P_{in} = 1.8 bar, but it is insignificant in terms of emissions. Soot emissions are also extremely low.

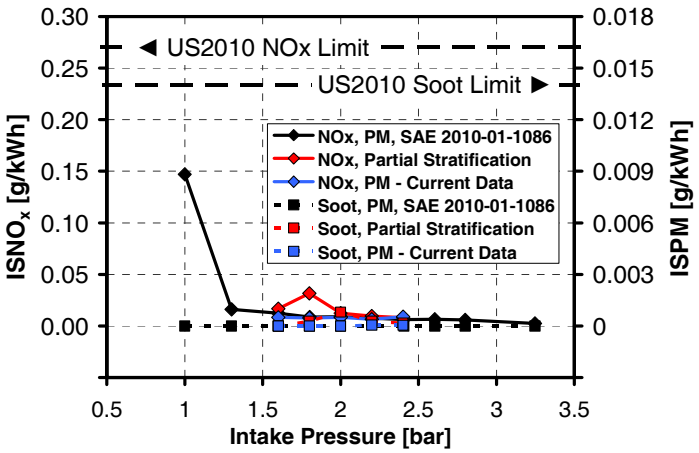

Figure 15. NOx emissions corresponding to the maximum load points presented in Fig. 13.

Figure 16 presents the indicated-thermal and combustion efficiencies and NOx emissions for the maximum load points presented in Figs. 13 and 14. Combustion efficiencies for P_{in} = 1.6 and 1.8 bar are similar to the premixed points, but they drop slightly below the premixed values for P_{in} = 2 and 2.2 bar. As mentioned previously, this is thought to be the result of insufficient oxygen in the richest stratified regions. The combustion efficiency falls even farther below the premixed values for P_{in} = 2.4 bar as excess oxygen reaches even lower levels (0.4%). Despite this modest drop in combustion efficiency, the thermal efficiency remains approximately the same as for premixed fueling even though the load is higher, mainly because CA50 can be more advanced with PFS.

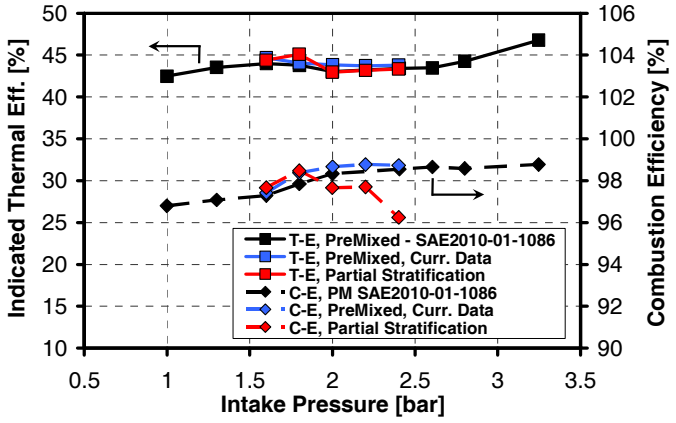

Figure 16. Indicated-thermal and combustion efficiencies corresponding to the maximum load points presented in Fig. 13.

INCREASING THERMAL EFFICIENCY WITH PFS

For boosted HCCI near the high-load limit, higher fueling rates typically have lower thermal efficiencies due to the need for greater timing retard and higher EGR levels, as discussed previously and shown in Fig. 11b. However, applying PFS allows higher loads with essentially the same thermal efficiency (Fig. 16). Therefore, switching from fully premixed to PFS fueling for the same load should provide an increase in thermal efficiency. To investigate this, premixed and PFS performance were compared at the same fueling rate and ringing intensity for several boost pressures and a variety loads from well-below the premixed high-load limit up to the limit.

Figure 17 shows the results of this study. As can be seen, for all cases, PFS fueling gave higher thermal efficiencies, which resulted in a higher $IMEP_g$ for the same fueling. The $IMEP_g$ values shown in Fig. 17 are the average $IMEP_g$ for each constant-fueling pair. Typically, PFS yielded a gain of about 1% in the thermal efficiency value compared to premixed fueling, corresponding to a fuel economy improvement of around 2 – 2.5%. As can be seen, the improvement in thermal efficiency varied with operating condition, ranging from about 0.3% to 1.6% for the data shown, corresponding to fuel economy improvements of 0.7 – 3.6%. Improvements were generally greater for $P_{in} \geq 2$ bar where ϕ-sensitivity is higher and PFS performance better. These thermal efficiency improvements occur mainly because PFS allows more advanced combustion phasing without excessive ringing.

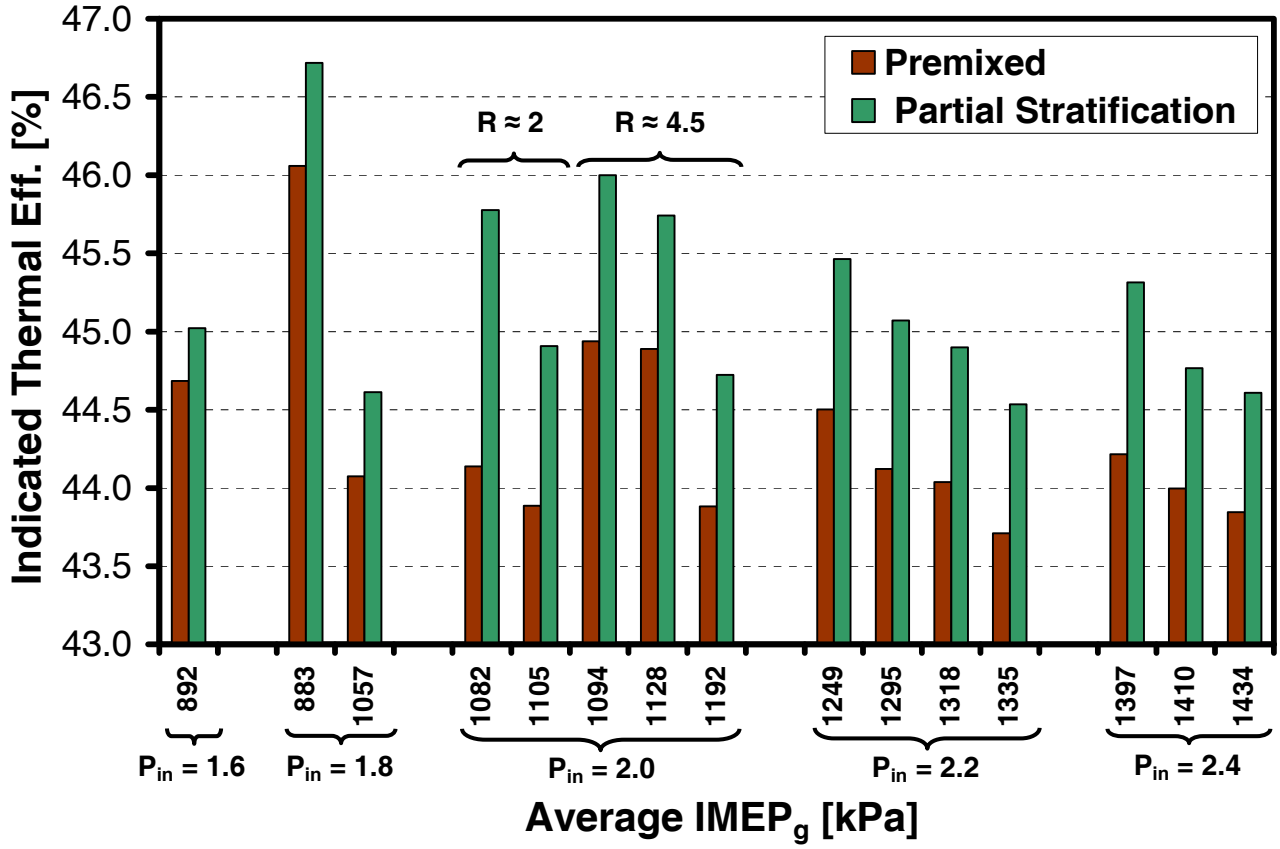

Figure 17. Comparison of indicated thermal efficiency for PFS and premixed operation for a range of loads and intake pressures. The "R" values shown above the P_{in} = 2 bar data indicate two ranges of ringing intensity. All other data are for ringing intensities of approximately 5 MW/m^2.

SUMMARY AND CONCLUSIONS

The application of partial fuel stratification (PFS) to reduce the heat-release rate (HRR), and therefore the knocking propensity, of intake-boosted HCCI engines has been systematically investigated. PFS is produced by premixing the majority of the fuel and then directly injecting the remainder (up to about 20%) in the latter part of the compression stroke using a GDI fuel injector. The study consists of four parts. First, the sensitivity of the fuel's autoignition to variations in equivalence ratio (ϕ-sensitivity) was measured for intake pressures (P_{in}) of 1 bar (naturally aspirated), 1.6, and 2 bar. The ϕ-sensitivity is a key parameter because PFS reduces the HRR by causing a staged combustion event as autoignition occurs sequentially down the equivalence ratio (ϕ) gradient. Second, the potential for PFS to produce a significant reduction in HRR was examined for P_{in} = 1 and 2 bar. This part includes an investigation of the effects of adjusting the in-cylinder ϕ-distribution by varying both the timing and amount of the directly injected fuel. Third, PFS was applied to boosted HCCI for intake pressures from 1.6 to 2.4 bar, to determine its effectiveness for extending the high-load limit. Fourth, comparative studies were conducted for a range operating conditions to determine the effectiveness of PFS for improving the thermal efficiency of boosted HCCI. The fuel was research-grade gasoline (RON = 91.7, MON 83.4). All data were taken at 1200 rpm, and the HCCI research engine was equipped with a compression-ratio 14 piston. For all high-load performance studies at boosted conditions, the intake temperature was held constant at 60°C, and combustion phasing was controlled by the addition of real or simulated EGR. The study produced the following results for the conditions studied:

1. The ϕ-sensitivity of gasoline varies substantially with intake pressure. For P_{in} = 1 bar (naturally aspirated), gasoline is not ϕ-sensitive, and PFS is not effective at reducing the HRR.
2. Under boosted conditions, the ϕ-sensitivity of gasoline increases greatly. For P_{in} = 1.6 bar, it shows moderate ϕ-sensitivity, and for P_{in} = 2 bar, gasoline has very strong ϕ-sensitivity.
3. With gasoline's strong ϕ-sensitivity at P_{in} = 2 bar, PFS is highly effective at reducing the HRR, and therefore, the maximum pressure-rise rate (PRR) and knocking propensity of HCCI combustion.
4. Both retarding the DI timing and/or increasing the DI fraction are effective for increasing the amount of mixture stratification and producing a greater reduction in the HRR and PRR.
5. Performance results show that PFS can extend the high-load limit of HCCI at P_{in} = 2 bar up to an $IMEP_g$ = 13.0 bar (near the oxygen-availability limit, with EGR ~ 41%), compared to a maximum $IMEP_g$ = 11.7 bar for premixed fueling.
6. For higher boost levels, P_{in} = 2.2 and 2.4 bar, PFS allowed fueling to be increased to the oxygen limit (EGR ~ 48 – 50%). However, PFS will not likely be of value for $P_{in} \geq 2.6$ bar, which is already oxygen limited for premixed fueling with this fuel (EGR = 52%) at the 1200 rpm condition studied.
7. PFS was less effective at extending the high-load limit at P_{in} = 1.6 and 1.8 bar, where the fuel is less ϕ-sensitive. For these conditions, the load could only be increased a few percent above the premixed limit using PFS, before reaching the knock/stability limit.
8. PFS is also effective for increasing the thermal efficiency of boosted HCCI over a range of operating conditions because it reduces the PRR, allowing more advanced combustion phasing without knock. For P_{in} = 1.6 – 2.4 bar, at a variety of fueling rates from well below the premixed high-load limit up to the limit, PFS increases the thermal efficiency, typically by an amount sufficient to give fuel economy improvements of 2 – 2.5%.
9. All PFS performance points examined showed extremely low NOx and soot emissions, well below US-2010 standards.

Overall, PFS can significantly reduce the PRR for gasoline-fueled, boosted HCCI, giving it strong potential for improving performance over a range of operating conditions, both by extending the high-load limit and by improving efficiency.

REFERENCES

1. Olsson, J-O, Tunestål, P., Johansson, B., Fiveland, S., Agama, J. R., and Assanis, D. N., "Compression Ratio Influence on Maximum Load of a Natural Gas-Fueled HCCI Engine", SAE paper 2002-01-0111, 2002.
2. Sjöberg, M., Dec, J. E., Babajimopoulos, A., and Assanis, D., "Comparing Enhanced Natural Thermal Stratification against Retarded Combustion Phasing for Smoothing of HCCI Heat-Release Rates," *SAE Transactions*, 113(3), pp. 1557-1575, paper 2004-01-2994, 2004.
3. Sjöberg, M. and Dec, J. E., "Influence of Fuel Autoignition Reactivity on the High-Load Limits of HCCI Engines," SAE paper 2008-01-0054, 2008.
4. Sjöberg, M. and Dec, J. E., "Comparing Late-cycle Autoignition Stability for Single- and Two-Stage Ignition Fuels in HCCI Engines," *Proceedings of the Combustion Institute*, Vol. 31, pp. 2895–2902, 2007.
5. Christensen, M., Johansson, B., Amnéus, P. and Mauss, F., "Supercharged Homogeneous Charge Compression Ignition," SAE paper 980787, 1998.
6. Christensen, M. and Johansson, B., "Supercharged Homogeneous Charge Compression Ignition (HCCI) with Exhaust Gas Recirculation and Pilot Fuel," SAE paper 2000-01-1835, 2000.
7. Olsson, J.-O., Tunestål, P., Haroldsson, G. and Johansson, B., "A Turbo-Charged Dual Fuel HCCI Engine," SAE paper 2001-01-1896, 2001.
8. Bessonette, P. W., Schleyer, C. H., Duffy, K. P., Hardy W. L., and Liechty, M. P. "Effects of Fuel Property Changes on Heavy-Duty HCCI Combustion," SAE paper 2007-01-0191, 2007.
9. Dec, J. E. and Yang, Y., "Boosted HCCI for High Power without Engine knock and with Ultra-Low NOx Emissions – using Conventional Gasoline," SAE paper 2010-01-1086, SAE International Congress, Detroit MI, April 2010.
10. Sjöberg, M. and Dec, J. E., "Smoothing HCCI Heat-Release Rates using Partial Fuel Stratification with Two-Stage Ignition Fuels," *SAE Transactions*, Vol. 115, Sec. 3, pp. 318-334, paper no. 2006-01-0629, 2006
11. Dec, J. E. and Sjöberg, M., "Isolating the Effects of Fuel Chemistry on Combustion Phasing in an HCCI Engine and the Potential of Fuel Stratification for Ignition Control," *SAE Transactions*, 113(4), pp. 239-257, SAE paper 2004-01-0557, 2004.
12. Dec, J. E. and Sjöberg, M., "A Parametric Study of HCCI Combustion – the Sources of Emissions at Low Loads and the Effects of GDI Fuel Injection," *SAE Transactions*, 112(3), pp. 1119-1141, SAE paper 2003-01-0752, 2003.
13. Y. Yang, J.E. Dec, N. Dronniou, and M. Sjöberg, "Tailoring HCCI Heat Release Rates with Partial Fuel Stratification: Comparison of Two-Stage and Single-Stage Ignition Fuels". Proceedings of the Combustion Institute, 2011. **33** (In Press).
14. Yang, Yi, Dec, J. E., Dronniou, N., Sjöberg, M. and Cannella, W. J., "Partial Fuel Stratification to Control HCCI Heat Release Rates: Fuel Composition and Other Factors Affecting Pre-Ignition Reaction of Two-Stage Ignition Fuels," submitted to the 2011 SAE International Congress, Paper offer number 11PFL-0706.
15. D. Dahl, M. Andersson, A. Berntsson, I. Denbratt, and L. Koopmans, "Reducing Pressure Fluctuations at High Loads by Means of Charge Stratification in HCCI Combustion with Negative Valve Overlap". SAE Paper No. 2009-01-1785, 2009.
16. Y. Wada and J. Senda, "Demonstrating the Potential of Mixture Distribution Control for Controlled Combustion and Emissions Reduction in Premixed Charge Compression Ignition Engines". SAE Paper No. 2009-01-0498, 2009.

17. Yang, Y., Dec, J. E., Dronniou, N., and Simmons, B., "Characteristics of Isopentanol as a Fuel for HCCI Engines," SAE paper 2010-01-2164, accepted for SAE 2010 Fall Powertrain, Fuels and Lubricants Meeting, San Diego, CA, October 25-27, 2010.
18. Sjöberg, M., Dec, J. E., and Hwang, W., "Thermodynamic and Chemical Effects of EGR and Its Constituents on HCCI Autoignition," *SAE Transactions* 116(3), SAE paper 2007-01-0207, 2007.
19. Heywood, J. B., Internal Combustion Engine Fundamentals, McGraw-Hill, New York, 1988.
20. Eng, J. A., "Characterization of Pressure Waves in HCCI Combustion", SAE Paper 2002-01-2859, 2002.
21. Snyder, J. A., Dronniou, N., Dec, J. E., and Hanson, R. K., "PLIF Measurements of Thermal Stratification in an HCCI Engine under Fired Operation," submitted to the 2011 SAE International Congress, Paper offer number 11PFL-0797.
22. Sjöberg, M. and Dec, J. E., "Combined Effects of Fuel-Type and Engine Speed on Intake Temperature Requirements and Completeness of Bulk-Gas Reactions for HCCI Combustion," SAE paper 2003-01-3173, 2003.
23. Sjöberg, M., Dec, J. E., and Cernansky, N. P., "The Potential of Thermal Stratification and Combustion Retard for Reducing Pressure-Rise Rates in HCCI Engines, based on Multi-Zone Modeling and Experiments," *SAE Transactions*, 114(3), pp. 236-251, SAE paper 2005-01-0113, 2005.
24. Dec, J. E. and Hwang, W., "Characterizing the Development of Thermal Stratification in an HCCI Engine Using Planar-Imaging Thermometry," *SAE Int. J. Engines*, **2**(1): 421-438, paper 2009-01-0650, 2009.
25. Dec, J. E., Sjöberg, M., and Hwang, W., "Isolating the Effects of EGR on HCCI Heat-Release Rates and NO_X Emissions," *SAE Int. J. Engines*, **2**(2): 58-70, 2010, SAE paper 2009-01-2665.
26. Sjöberg, M., Dec, J. E., "Influence of Fuel Autoignition Reactivity on the High-Load Limits of HCCI Engines", *SAE Int. J. Engines* 1(1): 39-58, SAE paper 2008-01-0054, 2008.
27. Risberg, P., Johansson, D., Andrae, J., Kalghatgi, G., Björnbom, P., and Ångström, H.-E., "The Influence of NO on the Combustion Phasing in an HCCI Engine", SAE Paper 2006-01-0416, 2006.
28. Sjöberg, M. and Dec, J. E., "Influence of EGR Quality and Unmixedness on the High-Load Limits of HCCI Engines," *SAE Int. J. Engines*, **2**(1): 492-510, paper 2009-01-0666, 2009.

CONTACT INFORMATION

Corresponding author: John E. Dec, Sandia National Laboratories, MS 9053, PO Box 969, Livermore, CA 94551-0969, USA.

ACKNOWLEDGMENTS

The authors would like to thank Kenneth St. Hilaire, David Cicone, Christopher Carlen and Gary Hubbard of Sandia National Laboratories for their dedicated support of the HCCI engine laboratory.

This work was performed at the Combustion Research Facility, Sandia National Laboratories, Livermore, CA. Support was provided by the U.S. Department of Energy, Office of Vehicle Technologies. Sandia is a multiprogram laboratory operated by the Sandia Corporation, a Lockheed Martin Company, for the United States Department of Energy's National Nuclear Security Administration under contract DE-AC04-94AL85000.

APPENDIX

The effects of PFS on other parameters for the DI timing and DI fraction sweeps in Figs. 6 -9.

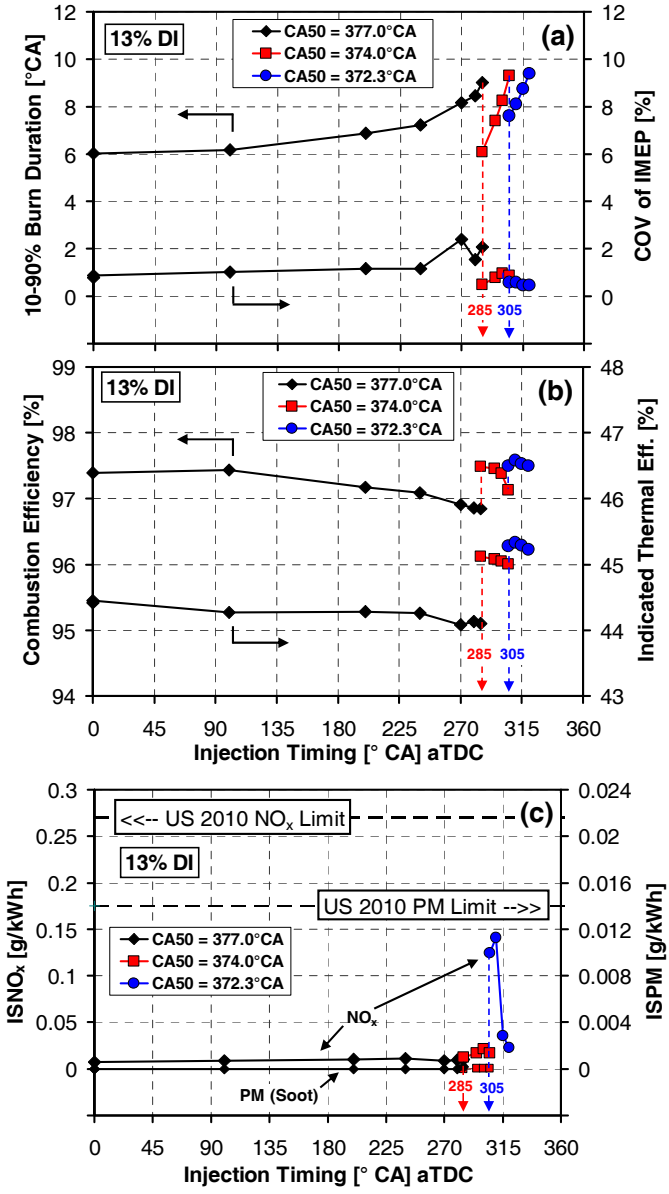

Figure A1. Parameters for PFS DI-timing sweep for P_{in} = 2 bar, ϕ_m = 0.44. (a) $IMEP_g$ and COV of $IMEP_g$, (b) combustion and thermal efficiency, (c) NOx and soot emissions. Note that no soot emissions data are available for the CA50 = 372.3° CA data.

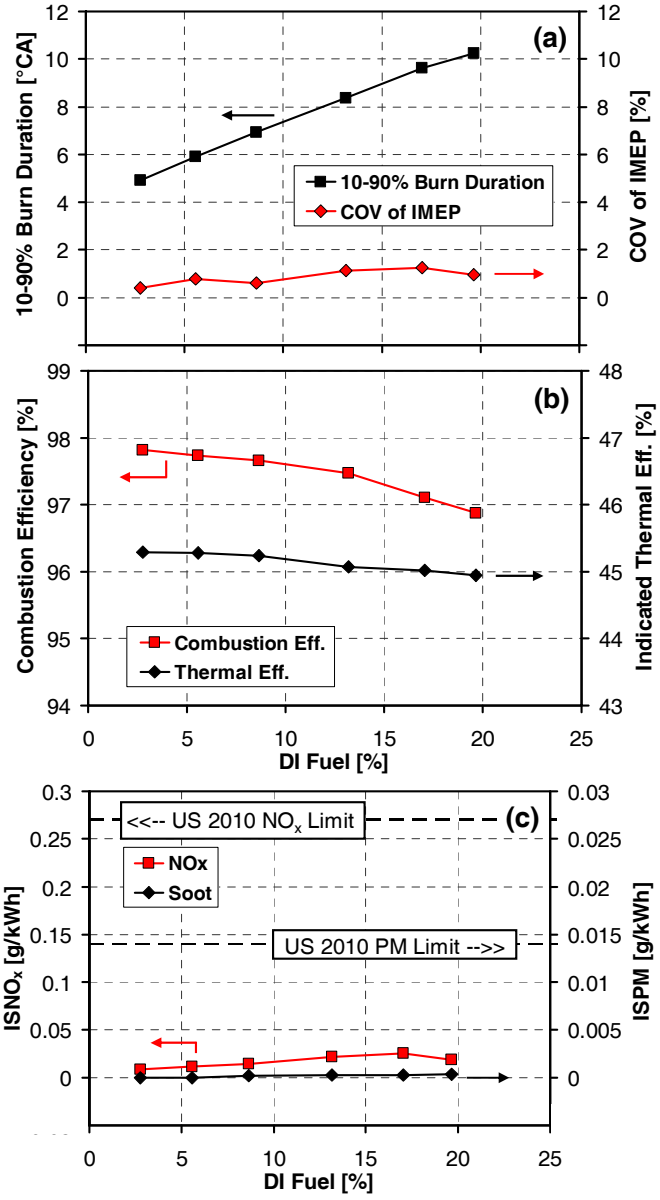

Figure A2. Parameters for PFS DI-fraction sweep for P_{in} = 2 bar, ϕ_m = 0.44. (a) $IMEP_g$ and COV of $IMEP_g$, (b) combustion and thermal efficiency, (c) NOx and soot emissions.